Chapter 2

Review of Literature

2.1 Introduction

In recent times, exponential population growth has emerged as a significant driving force propelling our societies towards unprecedented levels of urbanization and mechanization. Concurrently, the rapid rise in mechanization has revolutionized industries, enhancing productivity and efficiency across various sectors. However, this surge in demand for progress and convenience has necessitated the progressive utilization of energy resources. Our societies are faced with the crucial task of striking a delicate balance between meeting the increasing demand for energy and adopting sustainable practices to ensure a harmonious co-existence with our environment. Furthermore, this unprecedented increase in energy demand has given rise to legitimate concerns over the availability of finite fuel reserves. As consumption surges, there is a growing apprehension about the depletion of non-renewable resources and the potential consequences of an energy crisis. Simultaneously, heightened energy utilization has intensified environmental concerns, triggering debates on climate change, pollution, and ecological degradation. These pressing issues have propelled a global shift towards seeking alternative and sustainable energy sources, prompting investments in renewable technologies and energy efficiency initiatives to mitigate the environmental impact and ensure a more secure energy future for generations to come. Researchers and policymakers alike have turned their attention to biomass as a promising and sustainable source of energy, which can be converted into usable energy through various processes [1]. These include bioenergy technologies such as biofuels, biogas, and bioelectricity generation. Additionally, advancements in biomass gasification and pyrolysis techniques have garnered attention for their potential to produce cleaner energy with reduced greenhouse gas emissions. As efforts intensify to promote renewable energy solutions, the exploration of biomass as a viable and eco-friendly alternative has become a key focus in the quest for a more sustainable energy future. Collaborative research and policy initiatives are being devised to encourage the adoption of these pathways and technologies, fostering a transition towards a greener and more resilient energy landscape.

2.2 Various Waste Biomass and Bio-waste: Their Applicability in Pyrolysis

The thermo-chemical platform aims to efficiently produce bio-based fuels and co-products by employing processes like liquefaction and pyrolysis, followed by the refinement of bio-oils and gaseous intermediates. The thermo-chemical conversion process, such as pyrolysis, differs from biochemical or biological processes in the sense that a wide range of biomass materials can be utilized, including different bio-waste and pyrolysis doesn't require extensive pre-treatment of the biomass. In essence, pyrolysis is nearly indiscriminate in its choice of biomass, similar to combustion.

Bio-waste encompasses a broad spectrum of biological materials, including lignocellulosic resources such as wood chips and crop residues, industrial byproducts, municipal wastes, seeds, seed cakes, and seed covers, aquatic plants and algae, invasive weeds, and shrub species as indicated in **Table 2.1**.

Table 2.1: Types of waste biomass feedstocks utilized in pyrolysis

Biomass/Biowaste types	Biomass
Forest residues	Wood, bark, chips, and sawdust of trees such as pine, Australian oil mallee, white oak, beech, spruce, Poplar wood, Ulin Wood, Messua ferrea (Iron wood tree), etc.
Industrial wastes and Municipal wastes	Olive industry residues, palm shell, palm fiber, palm empty fruit branch, coffee ground, apricot pulp, peach pulp, tea factory wastes, rice husk, coir pith, Jute dust, Sewage sludge, Black liquor, etc.
Agricultural residues	Sesame stalk, Sunflower extracted bagasse, sugarcane bagasse, grape bagasse, rice straw, wheat straw, oat straw, cotton stalk, maize stalk, flex straw, corn stalk, Jute stick, tea stalks, Peanut shell, Spent mushroom, Hemp straw, Oil Palm Empty Fruit and Bunches, Mustard stalk, etc.
Seeds, Seed cakes, and seed covers	Neem seed, Cotton seed, Karanja seed, Mahua seed, Rapeseed, Jatropha seed, Niger seed, soybean cake, Pongamia, Cotton seed, Kusum, Miscanthus, Castor, Safflower, *cascabela thevetia*, Gulmohar seed, *Mesua ferrea* L., *Kayea assamica* seedcake
Aquatic plants and algae	Duckweed, Azolla, Water hyacinth, Water fern, Water lettuce, Ipomea, Microalgae chlorella, marine brown algae
Invasive weeds and shrub species	*Parthenium argentatum, Lantana camara*, *Siam weed, Ageratina adenophora, Prosopis juliflora, Lythrum salicaria, Lonicera japonica, Berberis thunbergia, Acer platanoides, Heracleum mantegazzianum,* tithonia, elephant grass, switchgrass, etc.

Numerous reports have highlighted the pyrolytic conversion of these diverse types of bio-waste into biofuel and by-products. Additionally, researchers have conducted analyses to assess their physicochemical properties and potential applications across various fields. Different waste biomass feedstocks with their physicochemical and biochemical properties have been listed in **Table 2.2**. Consequently, we will delve into a few studies that explore the pyrolytic conversion of different types of bio-waste for their utilization as a fuel source

Table 2.2: Physicochemical and biochemical properties of diverse waste biomass feedstocks

Sl. No	Biomass feedstock	Volatile matter	Fixed carbon	Ash	Moisture	Cellulose	Hemicellulose	Lignin	Extractives	C	H	N	O	S	References
Wood and Wood waste															
1	Poplar wood	-	-	1.86	-	-	-	-	-	44.55	6.56	0.05	46.60	0.38	[71]
2	Ulin Wood	74.32	22.83	2.85	-	-	-	-	-	49.28	5.64	0.30	44.78	-	[69]
3	Pine wood	81.27	15.49	3.24	-	-	-	-	-	46.69	5.89	0.0	47.42	-	[69]
4	Pinewood	83.01	14.30	0.35	2.35	-	-	-	-	47.4	6.1	0.1	46.4	0.1	[64]
5	*Messua ferrea* (Iron wood tree)	77.33	16.02	1.24	5.81	-	-	-	-	47.64	6.75	1.10	44.51	-	[205]
6	Saw dust	76.35	16.67	2.05	4.62	-	-	-	-	46.83	6.35	1.15	45.67	-	[205]
Agricultural wastes or Crop residues															
7	Sesame stalk	70.72	10.06	11.24	7.98	32.34	18.20	31.17	18.29	44.65	9.34	1.33	44.68	-	[63]
8	Rice straw	60.66	16.56	12.71	10.07	-	-	-	-	37.42	4.7	0.7	34.3	0.16	[64]
9	Peanut shell	72.74	23.06	2.05	2.15	-	-	-	-	49.90	6.6	0.8	38.5	0.2	[64]
10	Tea stalk	60.80	27.1	6.5	5.6	-	-	61.3	-	47.1	5.8	2.7	-	-	[58]
11	Paddy straw	11.6± 0.3	20.21 ± 0.2	12.49 ± 0.2	-	42± 1.65	23.5± 0.66	17.33± 2.11	17.16± .98	39.76± 0.1	5.38± 0.2	0.84± 0.2	-	-	[72]

12	Spent mushroom	12.7± 0.1	15.94 ± 0.1	9.96± 0.1	-	40.83± 0.76	19.3±1. 11	15.67± 1.11	24.2±2. 83	27.82± 0.2	4.00± 0.1	0.87± 0.2	-	-	[72]
13	Oat straw	66.70	18.8	6.9	7.6	-	-	-	-	43.97	6.16	0.66	48.95	0.11	[55]
14	Garlic outer peel	66.38	11.01	9.76	12.85	47.74	27.28	15.22	-	44.55	4.71	0.70	38.65	0.17	[43]
15	Garlic inner peel	65.59	13.09	6.30	15.03	51.48	30.72	11.50	-	47.51	4.91	1.75	37.89	0.45	[43]
16	Rice husk	62.23	13.83	23.93	-	11.78	31.60	18.96	-	35.0	4.9	0.7	59.1	0.3	[186]
17	Hemp straw	81.12	16.21	2.67	-	16.79	32.15	5.21	-	44.90	6.4	0.6	47.6	0.5	[186]
18	Corncob	-	-	2.1	6.3	31.7	3.4	31.7	-	42.90	6.40	0.60	-	0.29	[220]
19	Oreganum stalk	-	-	4.0	9.0	33.8	9.3	10.9	-	42.50	6.00	0.70	-	0.29	[220]
20	Oil Palm Empty Fruit Bunches	61	19.2	10.6	9.20	-	-	-	-	42.32	5.74	1.84	39.24	0.26	[200]
21	Rice husk	55.5	15.7	16.1	12.7	-	-	-	-	45.2	5.8	1.02	47.6	0.21	[200]
22	Cotton stalks	71.0	16.6	3.5	8.9	39.4	19.2	23.2	-	46.8	6.4	0.3	46.8	0.2	[201]
23	Mustard stalk	70.0	12.3	7.9	9.7	39.5	18.7	22.5	-	43.8	5.9	0.3	43.8	0.3	[201]
24	Sugarcane bagasse	76.0	9.6	4.4	10.0	36.6	18.7	19.8	-	43.2	6.2	0.4	43.2	0.8	[201]
	Industrial and municipal wastes														
25	Tea Factory waste	68.60	24.80	4.36	2.24	-	-	-	-	51.82	6.31	2.46	39.22	-	[181]
26	Coir pith	74.03± 0.34	10.59 ±0.34	6.72± 0.07	8.67± 0.06	-	-	-	-	45.57	6.28	1.66	46.49	-	[182]
27	Black liquor	53.92	37.20	3.12	5.76	-	-	-	-	34.12	4.21	0.41	32.99	5.60	[183]
28	Jute dust	72.11	12.90	9.65	5.34	60.08	10.56	4.62	13.09	43.71	6.18	1.38	48.75	-	[184]

29	Acrylonitrile butadiene styrene	98.13	0.46	1.41	-	-	-	-	-	83.63	13.68	0.00	-	0.15	[185]
30	Polyethylene	97.21	2.16	0.64	-	-	-	-	-	75.54	7.65	3.13	-	0.61	[185]
31	Polypropylene	98.54	1.26	0.20	-	-	-	-	-	72.38	8.14	1.94	-	0.12	[185]
32	Sewage sludge	45.05	8.95	46.0	-	-	-	-	-	25.3	4.2	3.3	66.7	0.5	[186]
	Oil bearing Seeds, seed covers, and seedcakes														
33	Miscanthus	76.16	7.55	5.49	10.8	13.63	43.34	26.29	17.62	-	-	-	-	-	[187]
34	Mahua	91.76	1.1	1.49	5.65	55.3	3.7	11.1	57.16	55.87	7.94	2.74	33.20	0.25	[188]
35	Karanja	89.23	2.0	1.5	7.27	62.7	4.2	25.5	53.19	53.04	7.32	3.94	35.53	0.17	[188]
36	Niger	86.13	1.3	6.6	5.97	45.9	9.8	28.3	39.75	50.96	7.13	4.05	37.7	0.29	[188]
37	Jatropha	86.5	5.0	4.0	4.5	7.81	40	29.6	19.32	-	-	-	-	-	[189]
38	Pongamia	78.1±0.24	10.3± 0.31	4.6± 0.13	7.0± 0.16	21.4± 0.99	26.8± 2.01	3.8± 0.23	-	43.98± 0.15	6.4± 0.12	3.9± 0.23	41.5± 0.21	0.24± 0.02	[190]
39	Gulmohar seed	75.56± 0.5	15.80 ±0.2	2.07± 0.12	7.09± 0.05	48.16± 0.13	27.22 ±0.13	14.06± 0.11	30.12± 0.40	53.5	6.93	6.99	32.55	-	[192]
40	*Cascabela thevetia (CT)*	78.05± 0.71	14.78 ±0.11	2.19± 0.14	4.97± 0.10	36±0.12	21.01± 0.16	15.23± 0.13	57.40± 0.60	54.93	9.99	3.33	31.07	0.66	[192]
41	CT seed cover	75.71	16.15	4.52	3.62	-	-	-	-	47.50	6.44	1.75	44.31	-	[193]
42	CT deoiled cake	73.81	16.82	4.20	5.10	-	-	-	-	46.08	7.20	6.43	40.29	-	[193]
43	*Mesua ferrea L.* deoiled cake (MFDC)	82.63± 0.66	8.46± 0.54	4.82± 0.47	4.08± 0.27	56.91	29	14.09	-	48.63	7.38	3.65	40.34	-	[197]

44	*Mesua ferrea* seed cover	76.83	18.20	1.17	3.80	-	-	-	-	47.5	5.43	1.15	45.9	-	[198]
45	*Pongamia glabra* seed cover	74.58	19.20	2.72	3.50	-	-	-	-	44.0	5.46	1.61	48.8	-	[198]
46	*Kayea assamica* seedcake	72.34	8.97	10.34	8.35	22.56± 0.58	20.25± 0.37	40.74± 0.31	16.45± 0.05	43.23	8.23	1.66	46.88	-	[155]
	Aquatic plants and algae														
47	*Ipomoea carnea*	70.30	17.65	4.65	8.40	38.81	23.98	33.20	4.01	42.54	6.22	0.56	50.55	-	[156]
48	*Lemna minor* (duckweed)	78.0	8.8	9.5	3.7	-	-	-		39.11	6.13	5.52	37.74	0.67	[157]
49	*Eichhornia crassipes*	-	-	19.2	93	-	-	-	2.6	34.5	4.9	45.7	0	-	[144]
50	*Eichhornia azurea*	-	-	14.5	90	-	-	-	6.0	40.6	4.5	47.1	0	-	[144]
51	*Nymphaea spp.*	-	-	13.0	89	-	-	-	2.4	38.3	3.9	42.5	0	-	[144]
52	*Azolla filiculoides*	88	4.4	7.3	11	-	-	-	-	46.2	7.4	3.0	43.2	0.2	[145]
53	*Water hyacinth*	77.8	0.4	21.8	9.5	-	-	-	-	35.0	6.5	0.8	-	1.4	[135]
54	*Sargassum tenerrium*	61.5	11.9	23.2	13.5	-	-	-	-	32.0	4.7	0.9	-	1.5	[135]
55	*Scenedesmus dimorphus*	51.45	31.13	17.33	0.083	-	-	-	-	52.0	6.21	8.75	31.92	-	[160]
56	Azolla	88.3	4.4	7.3	11.0	-	-	-	-	46.2	7.4	3.0	-	0.2	[135]
	Shrubs / Invasive plants														
57	*Arundo donax L.*	74.30	11.70	5.30	8.50	29.20	35.90	23.32	-	42.0	6.2	1.5	36.3	-	[100]

58	*Saccharum ravannae* L.	76.88	-	-	8.44	30.1	34.7	22.9	-	-	-	-	-	-	[84]
59	*Parthenium hysterophorus*	11.4± 0.1	13.23 ± 0.3	14.67 ± 0.1	-	23.77± 1.40	26.8±1. 61	22.06± 1.31	27.37± 0.80	37.03± 0.2	4.61± 0.2	1.40± 0.1	-	-	[72]
60	*Calotropis gigantea*	74.0	13.0	11.0	2.0	-	-	-	-	36.93	4.45	2.17	-	0.65	[73]
61	*Parthenium hysterophorus*	70 ± 0.6	14 ± 0.4	16 ± 0.8	-	-	-	-	-	35.56 ± 0.2	4.83 ± 0.2	2.83 ± 0.3	40.99 ± 0.3	0.32 ± 0.1	[75]
62	Reed Canary (*Phalaris arundinacea*)	80.9	3.67	8.82	6.6	-	-	-	-	40.42	4.95	1.41	53.22	<0.1	[54]
63	*Calotropis procera* stem	69.15	17.50	3.80	9.45	-	-	-	-	42.83	6.48	0.49	50.00	0.20	[2]
64	*Ageratum conyzoides* (goat weed)	71.02	19.23	4.61	5.14	30.05	38.33	10.41	21.21	34.44	4.88	0.46	59.92	0.30	[101]
65	*Xanthium strumarium*	-	-	4.913	6.231	40.89	21.32	26.19	0.455	43.69	5.98	0.94	49.40	-	[102]
66	*Calotropis procera*	71.83	16.83	2.02	9.32	-	-	-	-	44.96	6.28	0.92	47.60	0.24	[103]
67	Barnyard grass *(Echinochloa)*	70.77	20.89	7.06	1.28	-	-	-	-	44.24	6.12	0.86	41.02	0.71	[104]

68	Retinispora *(Chamaecyparis obtusa)*	77.47	18.87	2.09	1.57	-	-	-	-	36.34	6.21	0.29	54.58	0.50	[104]
69	*Cynodon dactylon*	70.89± 0.84	14.57 ± 0.17	11.34± 0.18	3.2±0.6	41.63± 0.26	19.28± 0.24	10.36± 0.18	7.10-10 20	44.86± 0.2	5.57±0.1	1.23±0.1	47.64±0.2	0.70±0.1	[105]
70	*Lantana camara*	78.5	19.3	2.2	-	48.2	28.9	20.6	2.3	-	-	-	-	-	[106]
71	*Mimosa pigra*	77.4	20.4	2.2	-	47.5	22.0	28.9	1.6	-	-	-	-	-	[106]
72	*Prosopis juliflora*	78.45	-	-	4.1	-	-	-	-	-	5.80-6.70	<0.5	-	-	[107]
73	*Lantana camara*	79.18	-	-	3.6	-	-	-	-	48.87	5.80-6.70	<0.5	44.82	-	[107]
	Animal wastes														
74	Goat manure	58.90	12.09	29.01	6.00	-	-	-	-	38.29	5.40	2.18	19.08	0.04	[108]
75	Swine manure	42.00	24.30	32.20	1.5	-	-	-	-	37.60	4.90	3.00	22.30	-	[109]
76	Horse manure	70.40	11.00	10.50	8.20	-	-	-	-	43.30	5.90	0.90	30.40	0.80	[110]
77	Chicken manure	69.23	19.13	11.64	-	-	-	-	-	31.54	4.52	3.34	60.18	0.56	[111]
78	Cattle Manure	70.5	15.3	14.2	5.6	28.1	11.9	12.9		40.89	6.72	1.51	50.12	-	[112]
79	Human feces	50.2	25.1	14.8	-	-	-	-	-	43.5	6.4	-	30.1	0.7	[113]
80	Pig manure	-	-	22.30	-	-	-	-	-	40.40	6.3	-	50.6	0.4	[114]
81	Yak manure	-	-		-	-	-	-	-	41.1 ± 0.1	6.1 ± 0.1	3.6 ± 0.1	39.7 ± 0.1	-	[115]
82	Cattle manure	53.43	5.59	40.68	0.30	-	-	-	-	24.80	3.00	2.90	45.30	1.30	[116]

2.3 Effect of Pyrolysis Parameters on Product Yield

Pyrolysis of biomass is a complex process in which biomass breaks down through various reactions involving heat and mass transfer. This thermal decomposition occurs under conditions with limited oxygen, leading to the formation of three main pyrolysis products: biochar, bio-oil, and gases. The amount and characteristics of these products are mainly influenced by factors like temperature, residence time of vapor, heating rate, particle size, as well as the composition of the biomass and the presence of inorganic elements in the feedstock. Understanding these factors is crucial for optimising the conditions to achieve the highest possible yield of the desired product. The influence of these pyrolysis parameters based on available literature sources has been discussed in the following section.

2.3.1 Feedstocks Composition

The choice of biomass feedstock plays a central role in determining both the quantity and characteristics of pyrolysis products. This intricate relationship between biomass composition, characterized by the relative proportions of organic constituents such as carbohydrates (hemicellulose, cellulose, and starch), lignin, fats, and proteins, as well as the presence of extractives and minerals, exerts a profound influence on the outcomes of pyrolysis [3]. The unique thermal decomposition behaviors of cellulose, hemicellulose, and lignin are critical factors in shaping the results of pyrolysis [4, 5]. Lignin, recognized for its exceptional thermal stability, predominantly yields solid char products during decomposition, while cellulose and hemicellulose contribute mainly to liquid and gaseous products [6-9]. Additionally, the presence of extractives affects the distribution of pyrolysis products, with higher extractive content favouring bio-oil production at the expense of gas and char formation [10].

Yang et al. [11] unveiled that hemicellulose and cellulose undergo rapid pyrolysis within specific temperature ranges, with hemicellulose decomposing primarily at 220–315°C and cellulose at 315–400°C. In contrast, lignin decomposition spans a wider temperature range, from 160 to 900°C, with only a portion of it volatilizing. These findings also emphasize the exothermic nature of hemicellulose and lignin pyrolysis reactions, contributing to increased solid residues, while the endothermic nature of

cellulose pyrolysis reactions is associated with rapid devolatilization, leaving fewer solid residues [12].

The significance of lignin content in determining pyrolysis outcomes for various biomass feedstocks was also investigated and Burhenne et al. [13] underscored that biomass with lower lignin content yielded the highest liquid product, whereas biomass with higher lignin content produced larger amounts of solid residues. This emphasizes the influence of lignin on the final temperature required to achieve maximum liquid product yield.

Furthermore, the carbon and heteroatom content in biomass significantly impacts fuel quality. Higher carbon content leads to increased char formation and higher calorific value, while lower mineral content promotes bio-oil production. However, the mineral content may also serve as a catalyst, influencing product distribution during pyrolysis [14, 15].

Moisture content in biomass is another pivotal factor. Elevated moisture content enhances bio-oil production but may impede the heating rate due to energy consumption during moisture evaporation [16-18]. In conclusion, comprehending the intricate interplay between biomass composition and the various factors affecting pyrolysis is imperative for optimizing the production of desired pyrolysis products.

2.3.2 Effect of Temperature

The temperature parameter is a critical factor in pyrolysis processes [19]. It significantly influences both the yield and characteristics of the resulting products [20, 21]. The temperature difference between the reactor and the feedstock serves as the driving force for heat transfer during pyrolysis, leading to increased thermal cracking as the temperature rises [22]. Generally, fast pyrolysis occurs within the temperature range of 400°C to 600°C, with the primary product being the liquid phase, specifically condensed product vapors, which typically constitute approximately 60% to 70% of the product [23-25]. It is noteworthy that while elevating the reaction temperature initially enhances the yield of liquid products, exceeding 500 °C exerts an adverse impact, resulting in a reduction in liquid yield [26, 27]. Typically, within the temperature range of 500 °C to 550 °C, the maximum bio-oil recovery is attainable, although this may exhibit variability depending on the feedstock. Beyond this temperature threshold, the bio-oil yield typically diminishes due to incomplete reactions at lower temperatures and an

escalation in secondary reactions involving heavy molecular-weight compounds in the pyrolysis vapors at higher temperatures. This leads to a decrease in bio-oil yield and an increase in gas production [27].

In the context of solid products, it is essential to note that elevating the temperature has an adverse effect on biochar yield. This is attributed to a gradual reduction in the output of solid residue [28-30]. This reduction primarily stems from the thermal cracking of high-molecular-weight hydrocarbons and the devolatilization of the primary char [31-33]. It is important to emphasize that the optimum biochar yield is typically attained at lower temperatures, specifically below 400°C. Beyond the critical threshold of 600°C, there is an observable increase in the production of gaseous products, primarily due to the secondary decomposition of char and oil [34-36].

Furthermore, temperature significantly influences the chemical properties of both biochar and bio-oil. As temperature rises, the pH value increases due to the elevated concentration of alkali salts derived from organic materials [37- 40]. Concurrently, the carbon content in both biochar and bio-oil rises, while the levels of oxygen and hydrogen decrease relative to the carbon content [41, 42]. High temperatures foster the formation of polycyclic aromatic hydrocarbons (PAHs), including pyrene, phenanthrene, anthracene, and naphthalene, primarily due to decarboxylation and dehydration reactions [5]. Additionally, a significant decrease in organic functional groups with increasing final temperature was also observed, although these groups remained stable in the liquid phase [44].

2.3.3 Heating Rate

The rate at which biomass is heated within a pyrolysis reactor is a critical parameter that profoundly affects the yield of bio-oil. This factor has a significant impact on the composition of pyrolysis products, and its significance is particularly pronounced in fast pyrolysis, where the production of liquid products exceeds that of conventional pyrolysis processes. Rapid heating rates play a pivotal role in facilitating the rapid and endothermic decomposition of biomass, resulting in an increased production of gases and liquids. The rapid fragmentation of biomass induced by high heating rates enhances the production of volatile compounds, which can be attributed to additional tar decomposition [45]. Rapid heating rates alleviate heat and mass transfer limitations while promoting the abundance of volatile compounds through the swift endothermic decomposition of

biomass, thus reducing the time available for secondary reactions [46, 47]. Thus, a higher heating rate has been considered as it is the preferred choice for maximizing liquid yield.

In order to comprehensively understand the impact of heating rate on pyrolysis liquid yield, numerous experiments have been conducted by research groups globally [48-52, 87]. Increasing the heating rate maximizes the rate of mass loss in the biomass feedstock [53]. Conversely, a lower heating rate results in an increased production of biochar, primarily due to the reduced occurrence of secondary pyrolysis reactions and thermal cracking [33]. Several investigations [40, 51, 56] emphasize a reduction in biochar yield with an increase in heating rate. Higher heating rates offer advantages in terms of product quality due to lower oxygen and moisture content, as well as reduced secondary reactions [48, 57].

2.3.4 Effect of Particle Size

Particle size plays a significant role in determining the yield of pyrolysis products. As particle size increases, it tends to create larger temperature gradients within the particle. Consequently, the core temperature remains lower than the surface temperature. This effect often leads to higher char yields but can reduce gas and oil yields [59, 60]. Larger particles inherently require higher apparent activation energies, primarily due to heat transfer limitations.

In contrast, smaller particles offer a higher surface area that promotes interactions with the pyrolysis medium. This facilitates the formation of volatile products that can exit the biomass matrix without significant secondary reactions [53]. However, in a study conducted by Beaumont and Schwob [61], it was demonstrated that for slow pyrolysis, particle size has minimal influence on product yield. Given the inherently poor thermal conductivity of biomass, a preference for very small biomass particles is essential to enable rapid heating and, consequently, achieve high bio-oil yield. While pyrolysis reactors can achieve high heating rates, the low thermal conductivity of biomass restricts the extent of temperature gradients throughout the particle.

Additionally, Shen et al. [62] showed that particle size has a significant effect on the yield and composition of bio-oil. They documented that increasing biomass particle size corresponds to higher water content in the resulting bio-oil. Salehi et al. [19] investigated the impact of feedstock particle size on the distribution and quality of liquid and char products derived from the pyrolysis of sawdust within a fluidized-bed reactor.

The study encompassed a temperature range of 425-550 °C and categorized particle sizes into three groups: <590 μm, 590-1000 μm, and 1000-1400 μm. They revealed that the highest yield of bio-oil, approximately 62% by weight, was obtained when the pyrolysis was conducted at 500 °C using sawdust particles smaller than 590 μm. It is worth highlighting that, under these conditions, the bio-oil had the lowest water content, which is a key consideration in optimizing the quality of the bio-oil product. In another study, the optimal particle size range for bio-oil production while keeping water content low is 0.5-1.4 mm [221]. The study of Santiago et al. showed that particles larger than 0.5 mm appear not to be completely pyrolyzed, contrary to particles with a diameter between 0.250 mm and 0.355 mm, at 1000 °C [222]. However, Varma and Mondal [117] obtained maximum bio-oil from pine needles at a pyrolysis temperature of 550 °C with particle size between 0.6-1 mm. Suriapparao, V. and Vinu, R. [88], in 2018 observed that fast pyrolysis product yields and composition are influenced by particle size. They found that the yield of phenolics and linear hydrocarbons decreased, while gas production (CO and CO_2) increased with larger particle sizes. Interestingly, medium-sized particles (362.5 and 512.5 μm) yielded the highest amount of aromatics.

Hence, from the earlier investigation into the influence of particle size, it can be deduced that the most effective particle dimensions for enhancing pyrolysis product yields and composition depend on both the particular pyrolysis technology used as well as the intrinsic traits of the biomass under consideration.

2.3.5 Effect of Inert Gas Flow Rate

The residence time of vapor within a pyrolysis reactor is a critical factor in determining the type and composition of pyrolysis products. The interaction between hot pyrolysis vapors and the surrounding solid environment leads to the exothermic reaction, forming char. In order to minimize the impact of char formation, it is essential to optimize process parameters that enhance rapid mass transfer. Strategies for achieving this include employing vacuum pyrolysis, ensuring the swift removal of pyrolytic vapors, and using a smaller particle size for the feedstock [59]. To facilitate these objectives, inert gases like N_2, Argon, and water vapor are commonly employed. The use of inert gas flow serves a dual purpose: it reduces the residence time of hot pyrolytic vapours inside the reactor; minimizing secondary reactions such as thermal cracking, re-polymerization, and recondensation, and thus maximizing the yield of liquid products [48]. However, it is

crucial to note that while inert gas flow removes hot pyrolytic vapors from the reaction zone, rapid quenching is also necessary to prevent the degradation of valuable initial reaction products, as highlighted by Maggi and Delmon [65].

Aladin et al. [173] observed the impact of N_2 flow rate into the pyrolysis reactor at a rate of 1 l/min using raw materials derived from wood sawdust biomass waste, with a pyrolysis time of 2 hours and a pyrolysis temperature of 400°C. The results showed that the yield of liquid smoke as well as the quality of charcoal was better when nitrogen gas flow was employed compared to when it was not used. Putun et al. [66] observed only a modest ~3% increase in liquid yield (from 27.77% to 30.23%) when increasing the N_2 gas flow from 50 ml/min to 200 ml/min, with a slight decrease in pyrolytic oil yield occurring at 400 ml/min. Similar observations were made by Acikgoz et al. [67] and Demiral and Şensöz [68] within the range of 50-100 cm^3/min and 50-150 cm^3/min nitrogen flow rates, respectively, resulting in modest increases in pyrolytic oil production. These studies collectively present a nuanced understanding of the impact of nitrogen gas flow rates on the pyrolysis of various biomass feedstocks. While some observed modest increases in liquid yield with incremental nitrogen flow, others noted diminishing returns and even a decrease in liquid product yield at higher flow rates. This inconsistency across studies underscores the sensitivity of pyrolysis processes to nitrogen flow dynamics. Notably, Sensoz and Angin [51] found that the relationship between bio-oil yield and nitrogen flow is not strictly linear, and has an optimum flow rate for maximum yield. The bio-oil yield increased from 33.8% to 36.1% with a sweep gas flow rate of 100 cm^3/min but decreased to 33.0% with a flow rate of 200 cm^3/min. Similarly, Mohammed et al [70] investigated the effects of nitrogen flow rate (ranging from 20 to 60 mL/min) and reaction temperature (from 400 to 600 °C) in the pyrolysis of Napier grass stem. The results indicated that the yield of bio-oil and biochar decreased as the nitrogen flow rate exceeded 30 mL/min, while the gas yield increased. Thus, usually low gas velocity is sufficient to achieve maximum liquid product yield, as higher gas velocities may lead to volatiles leaving the system without effective condensation, resulting in increased gas formation [5]. Saif et al. [174] achieved a maximum bio-oil yield of 45 wt% through sugarcane bagasse pyrolysis in a semi-batch reactor. This yield was obtained at 500 °C with a particle size of 0.5-1 mm and a nitrogen flow rate of 200 cm^3/min. Their study revealed that increasing the nitrogen flow rate from 100 to 200 cm cm^3/min boosted bio-oil yield. However, further increases beyond 200 cm cm^3/min resulted in a decrease in yield. . The results collectively suggest that the selection of a sweeping gas flow rate is a critical

parameter in optimizing pyrolysis processes, with too high a flow potentially leading to reduced liquid product yields due to ineffective volatile condensation. Overall, the variations in outcomes underscore the complexity of the interplay between nitrogen flow, reaction conditions, and biomass composition in pyrolysis systems.

2.4 Biochemical Components of Biomass and Pyrolysis Mechanism

The pyrolysis of biomass involves breaking down complex organic molecules into simpler molecules, which can be further processed into products such as condensable vapours i.e. bio-oil, biochar, and gases. In this process, numerous reactions, including dehydration, depolymerization, isomerization, aromatization, decarboxylation, and charring, occur concurrently and sequentially. The pyrolysis of biomass generally consists of three main stages: initial evaporation of free moisture, primary decomposition, and secondary reactions (oil cracking and re-polymerization). The pyrolysis reaction mechanism is complex and depends on various factors. A few of these have already been mentioned in this chapter, such as temperature, pressure, heating rate, and residence time. The possible reaction with the desirable end-product of the pyrolysis process can be depicted as [74]:

$$\text{Biomass} \xrightarrow[\text{Inert atmosphere}]{\Delta} \text{Liquid (Organic+ Aqueous)} + \text{Solid char (FC, VM, Ash)} + \text{Gas } (CO_2, CO, H_2, CH_4)$$

(VM: Volatile Matter, FC: Fixed carbon)

Biomass pyrolysis can be divided into three stages which can be explained as follows [59]:

During the first stage, internal rearrangements occur, including water elimination, bond breakage, and the formation of free radicals, carbonyl, carboxyl, and hydro-peroxide groups like:

Biomass → Water + non-reacted residue

The second stage corresponds to the primary decomposition process, which occurs rapidly and produces pyrolysis products as follows:

Non reacted residue → (Volatile + Gases) + $(Char)_{primary}$

In the third stage, char obtained at the above steps decomposes slowly into a carbon-rich residual solid form, resulting in secondary charring as:

$(Char)_{primary}$ → (Volatile + Gases) + $(Char)_{secondary}$

Lignocellulosic biomass, a composite of hemicellulose, cellulose, and lignin, exhibits an uneven distribution within the cell wall. Cellulose forms tough microfibers, serving as the structural component, with amorphous hemicellulose and lignin filling the inner spaces. Interactions occur through hydrogen bonds between cellulose and hemicellulose or lignin, and a combination of hydrogen and covalent bonds between hemicellulose and lignin. This leads to the formation of lignin-carbohydrate complexes, resulting in residual fragments of carbohydrates or lignin in extracted samples.

The thermal degradation order of the major biomass constituents is as follows [3]: Hemicelluloses > Cellulose > lignin. Biomass pyrolysis is a complex process influenced by the decomposition of these components, varying reaction mechanisms, and rates, all of which depend on thermal processing conditions and reactor designs [40]. Interactions between hemicellulose and lignin influence the production of lignin-derived phenols and hydrocarbons [56]. The cellulose-hemicellulose interaction has a lesser impact on pyrolysis product formation and distribution [57]. During biomass pyrolysis, a large number of reactions take place in parallel and series, including dehydration, depolymerisation, isomerization, aromatization, decarboxylation, and charring [48].

Both endothermic and exothermic reactions occur for biomass pyrolysis, with cellulose pyrolysis being endothermic and lignin pyrolysis exothermic. Among the three components, pyrolysis of cellulose has been extensively analyzed and understood [9], with various models proposed to describe the reactions involved [12, 77-79]. These models, such as the Broido-Shafizadeh model, Waterloo model, and Varhegyi-Antal model highlight the competition between anhydrosugar formation and char production reactions during cellulose pyrolysis. While all three models concur on the competition between anhydrosugar formation through depolymerization and char formation reactions, distinctions can still be identified among these three mechanisms.

2.5 Pyrolysis of Lignocellulosic Biomass

Lignocellulosic biomass, a readily abundant and cost-effective sustainable carbon source, presents a promising feedstock to produce renewable fuels and commodity chemicals [85]. Lignocellulosic materials comprise biopolymers with diverse cell types, characterized by the presence of cellulose, hemicelluloses, and lignin within their cell walls, which have been discussed in the above section. Their intricate structure and the economic challenges associated with separating these components can hinder their

utilization as feedstock. Notably, pyrolysis stands as one of the earliest and simplest technologies used to convert lignocellulosic materials into an alternative class of fuels and chemicals [86].

The following studies examine various aspects of lignocellulosic biomass pyrolysis:

Yorgun et al. [20] reported the pyrolytic conversion of sunflower-extracted bagasse in a fixed bed reactor over a temperature range of 400–700 ºC and a heating rate of 7–40 ºC/min. The study explored the effects of temperature, heating rate, particle size, and atmosphere on product yields and chemical compositions. The highest oil yield of 23 wt.% was obtained under the N_2 atmosphere at a pyrolysis temperature of 550 ºC and a heating rate of 7 ºC/min. The chemical characterization indicated that the feedstock had the potential as a valuable source of fuel and chemicals.

Ucar and Karagoz, [90] performed slow pyrolysis experiments on pomegranate seeds within a temperature range of 400–800 ºC. They found that maximum liquid yields were obtained at temperatures of 500 and 600 ºC, and the bio-oils contained phenols, alkyl-benzenes, and high levels of non-aromatic hydrocarbons in water fractions. Also, the composition of gaseous products was found to contain CO_2, CO, CH_4, and hydrocarbons from C_2 to C_7 and H_2S. The resulting biochar showed promise as a carbon-rich fuel with high bulk densities and calorific values.

Nayan et al. [91] explored the pyrolysis of Karanja (*Pongamia glabra*) seeds in a semi-batch mode, varying temperatures from 450–550 ºC and a heating rate of 20 ºC/min. Analysis of the liquid product revealed the presence of alkanes, alkenes, ketones, carboxylic acids, and aromatic rings. GC-MS indicated hydrocarbons with carbon chains ranging from 14 to 31 atoms. The pyrolysis liquid exhibited physical properties closely resembling a mixture of diesel and petrol.

Nayan et al. [92] reported the pyrolysis of neem seeds in a semi-batch reactor, varying temperatures from 400–500 ºC with a heating rate of 20 ºC/min. FTIR analysis revealed alkanes, alkenes, ketones, carboxylic acids, and amines in the liquid products, with key constituents including octadecanenitrile, oleanitrile, 9-octadecenoic acid methyl ester, and stearic acid methyl ester. The resulting liquid product demonstrated potential for use as valuable chemicals.

Park et al. [94] in 2019, conducted fast pyrolysis of Larch sawdust, studying the influence of temperature, inlet gas velocity, feeding rate, and particle size on product yield and pyrolysis oil quality in a Conical spouted bed reactor. The highest pyrolysis oil yield

of 54.6 wt % was achieved at a reaction temperature of 500 °C, an inlet gas velocity of 4.75 m/s, a biomass feeding rate of 1.5 kg/h, and a particle size of 0.5–1.4 mm. Operating conditions affecting pyrolysis oil yield were ranked as (1) biomass particle size, (2) reaction temperature, (3) biomass feeding rate, and (4) inlet gas velocity.

In 2021, Hu et al. [95], investigated the effects of pyrolysis parameters (temperature, residence time, and heating rate) on the distribution of pyrolysis products from Miscanthus samples using Py/GC-MS. Their results showed that pyrolysis products from Miscanthus consisted primarily of ketones, aldehydes, phenols, heterocyclic compounds, and aromatic compounds. Large-scale pyrolysis of Miscanthus commenced at 400 °C, with pyrolysis products from Miscanthus reaching a maximum relative content of 98.34% at 700 °C.

The above-mentioned are a few examples of the pyrolytic valorization of lignocellulosic bio-waste, which has garnered increasing attention due to its manifold advantages from both energy and environmental standpoints.

2.5.1 Pyrolysis of Weed Biomass

In order to explore the potential of harnessing various invasive weed species for energy and chemical recovery, several studies have investigated the use of these weedy species in pyrolysis processes, including the effect of operating conditions on product formation, and characterization of the products obtained. A selection of these studies is discussed below:

Muradov et al. [96] conducted experiments focused on pyrolysis of *Lemna minor*. Their research examined the impact of temperature, residence time, and sweep gas flow rate on the yields of pyrolytic products. Their findings highlighted that temperature had a significant effect on the quantities of products, whereas residence time had a negligible influence on both yield and composition.

Promdee and Vitidsant [97] investigated the thermal degradation of cogongrass (*Imperata cylindrica*) at various temperatures (400 °C, 450 °C, and 500 °C). They discovered that the highest biochar yield (25 wt.%) was achieved at 400 °C, while the highest oil production (33.67%) occurred at 500 °C. The bio-oil contained oxygenated compounds such as phenols, hydroxyl, and carboxyl groups, suggesting its potential as a fuel source following further processing through thermal or catalytic cracking methods.

Aysu and Durak [225] conducted research on the thermochemical conversion of *Datura stramonium L*., employing both supercritical liquefaction and pyrolysis processes. In the liquefaction experiments, they used a cylindrical reactor with organic solvents (isopropanol and acetone) under supercritical conditions, both with and without catalysts (zinc oxide and calcium hydroxide) at temperatures of 275°C, 300°C, and 325°C. For the pyrolysis experiments, they utilized a fixed-bed tubular reactor at temperatures of 400°C, 500°C, and 600°C, with a constant heating rate. The study investigated the influence of process variables, including temperature and catalyst, on product yields. The composition of bio-oils from liquefaction and pyrolysis was compared and evaluated. Analysis of the liquids obtained at 300°C during liquefaction and at 500°C during pyrolysis was conducted using techniques such as elemental analysis, GC–MS, and FT-IR. The results identified 102 and 87 different types of compounds in acetone and isopropanol, respectively, while pyrolysis liquids contained 57 different types of compounds. Bio-oils from liquefaction consist of various organic compounds, including aromatics, nitrogenated, and oxygenated compounds, with phenolics being the primary components in pyrolysis liquids.

Saikia et al. [100] in 2015 investigated the effects of pyrolysis process parameters on the perennial grass species *Arundo donax L*. in a fixed-bed reactor. In their research, bio-oil yield achieved a peak of 26.18% at conditions of 500 °C, a heating rate of 40 ºC/min, and a gas flow rate of 150 ml/min. The resulting bio-oil had an H/C atomic ratio of 1.79 and a heating value of 24.70 MJ/kg. The biochar, produced under optimized conditions, exhibited a calorific value of 24.21 MJ/kg and a porous structure. In 2019, Oginni and Singh [226] also pyrolyzed *Arundo donax* in a batch reactor at 500 °C for 30 minutes and obtained 30.12% biochar, 45.62% bio-oil, and 24.26% non-condensable gases. The biomass and biochar had calorific values of 18.96 and 29.51 MJ/kg, respectively, which are different from the study conducted by Saikia et al. 2015 [100]. The biochar was alkaline, making it suitable for soil amendment, while the bio-oil was acidic and would require further processing. The non-condensable gases were primarily composed of CO, CO_2, O_2, and CH_4. The viscosity of the bio-oil decreased with increasing temperature.

Mundike et al. [106] conducted pyrolysis experiments on invasive non-indigenous plants, *Lantana camara* (LC) and *Mimosa pigra* (MP), at a milligram scale to assess the effects of temperature on char yield and higher heating value (HHV). They obtained

maximized HHVs of 30.03 MJ/kg (at 525°C) for LC and 31.01 MJ/kg (at 580°C) for MP. Higher char yields and HHVs for MP were attributed to its increased lignin content. Scaling up the process promoted secondary char formation, consequently increasing HHVs to 30.82 MJ/kg for LC and 31.61 MJ/kg for MP. The analysis of incondensable gas showed that temperature increases beyond preferred values led to dehydrogenation, decreasing HHV.

Bhattacharjee and Biswas, [99] in 2018 conducted a study on the fast pyrolysis of *Alternanthera philoxeroides* to evaluate its potential as a fuel source. Their research revealed that the highest bio-oil yield was achieved at a temperature of 450 °C, a heating rate of 50 °C/min, and a nitrogen gas flow rate of 0.2 L/min. The maximum liquid yield reached 40.10% at a sweeping gas flow rate of 0.1 L/min at 450 °C, with a constant heating rate of 25 °C/min. Bio-oil yield increased to 42.28% when the sweeping gas flow rate was adjusted to 0.2 L/min with the same heating rate. Further variation in the heating rate led to a bio-oil yield of 43.15% at 50 °C/min. Gas chromatography-mass spectrometry (GC-MS) and Fourier-transform infrared spectroscopy (FT-IR) analysis indicated higher percentages of phenol and oxygenated compounds in the bio-oil. Remarkably, the biochar exhibited a higher heating value of 20.41 MJ/kg, surpassing that of the bio-oil (8.88 MJ/kg) due to the presence of oxygenated compounds. Bio-oil was recommended for chemical synthesis, while the high surface area of biochar made it suitable for use as an adsorbent.

In 2020, Bhattacharjee and Biswas [101] also investigated the pyrolysis of *Ageratum conyzoides* (goat weed) in a semi-batch reactor over a temperature range of 350°C to 600°C, varying heating rates from 25°C/min to 100°C/min, and sweeping gas (N_2) flow rates ranging from 0.1 L/min to 0.5 L/min. They achieved the maximum pyrolytic oil yield of 37.55 mass% at a temperature of 525°C, with a constant heating rate and a sweeping gas flow rate of 75 °C/min and 0.2 L/min, respectively. The empirical formula of *A. conyzoides* pyrolytic oil and biochar was found to be $CH_{1.32}O_{0.82}$ and $CH_{0.82}O_{0.44}$, with high heating values of 17.79 MJ/kg and 22.93 MJ/kg, respectively. The presence of various hydrocarbon compounds in the pyrolytic oil makes it suitable for the production of chemicals, while the biochar's high alkalinity and carbonaceous nature make it suitable for soil modification or use as a solid fuel. The pyrolysis gas had a gross calorific value of 5.32 MJ/m^3 and could be utilized as an alternative gaseous energy source.

Qurat-ul-Ain et al. [229] investigated the utilization of the noxious weed *Parthenium hysterophorus* as a feedstock for pyrolysis at varying temperatures of 300, 450, and 600 °C. Temperature significantly influenced the yield and properties of pyrolysis products, including char, syngas, and bio-oil. The biochar yield decreased from 61% to 37% as the temperature increased from 300 to 600 °C, while the yield of gas and oil increased with higher temperatures. It was observed that the pH, conductivity, fixed carbon, ash content, bulk density, and specific surface area of the biochar increased with rising temperature, while cation exchange capacity, calorific value, volatile matter, hydrogen, nitrogen, and oxygen content decreased. The number of compounds decreased, but the proportion of aromatic compounds increased with higher temperatures.

Aquatic weeds are also considered as potential feedstock for thermochemical valorization. An undesired aquatic weed *Ipomoea carnea* had been used as feedstock by Saikia et al. [156] for the production of bio-oil, using thermal pyrolysis at temperatures ranging from 350°C to 600°C with a heating rate of 10°C/min. The maximum bio-oil yield was 41.17%, with 11.45% being the oil phase, achieved at a pyrolysis temperature of 550°C. The bio-oil contained various hydrocarbons and alcohols. The H/C molar ratio (1.49) of the bio-oil was found to be comparable to petroleum-derived diesel. However, the presence of oxygen (35.86%) in the form of oxygenates, especially organic acids, made the bio-oil acidic and required further processing for use in internal combustion engines. Gusain and Suthar, [98] explored the potential of aquatic weeds, including *Lemna gibba, L. minor, Pistia stratiotes,* and *Eichhornia sp*., as a fuel source in their study [98]. From FTIR analysis they confirmed the presence of high-energy molecules in these aquatic plants. Proximate analysis results indicated their suitability for production of ethanol, butanol, biodiesel, and more, thanks to their low ash content, high heating value, and fixed carbon. Among the above-mentioned species, *Eichhornia sp*. has been mostly studied for pyrolytic conversion. Santos et al. [144] evaluated the potential of invasive aquatic plants, including *Eichhornia crassipes* (water hyacinth), *Eichhornia azurea*, and *Nymphaea spp*., as sources of lignocellulosic biomass for bio-oil production using a micropyrolysis reactor at 500°C. They collected the bio-oil using an adsorbent and eluted it with various solvents, achieving the best recovery with tetrahydrofuran. Analysis of the bio-oil solutions using GC-MS revealed the presence of glycerol, o-benzenediol, p-benzenediol, arabinoic acid, levoglucosan, and hexadecanoic acid as the main compounds. Similarly, Wauton & Ogbeide [232] also identified major compounds in the

bio-oil of water hyacinth as phenols, alcohols, carboxylic acids, ketones, quinones, alkenes, alkanes, aldehydes, and aromatics. The bio-oil exhibited specific fuel properties, such as pH, water content, flash point, density, viscosity, and pour point, with values of 2.93, 58.58%, 220°C, 1004.3 kg/m^3, 19.8 cSt, and -15°C, respectively. The higher heating value of the bio-oil was determined to be 28.35 MJ/kg, marking a significant improvement over the original feedstock. Huang et al. [233] also evaluated the potential of different portions of water hyacinth, i.e., its roots (WHR), stems, and leaves (WHSL) for biofuel production by assessing their physicochemical properties, pyrolysis performance, kinetics, and thermodynamics. The primary pyrolysis temperature for the biomass ranged from 200 to 600 °C. The main gases produced from WHR and WHSL pyrolysis included CO_2, CO, SO_2, H_2O, and CH_4. The primary pyrolytic by-products were phenols (19.2%) and furans (12.4%) for WHR and nitrides (11.9%) and phenols (10%) for WHSL. In a recent study (2023) on water hyacinth, Malagón et al. [224] obtained bio-oil with the composition of 44% hydrocarbons, 27% aromatic hydrocarbons, 6% alcohols, and phenols, 4% acids, and 19% aldehydes, ketones, ethers, nitriles, and other compounds, emerged bio-oil as a potential candidate for refined chemical product production. Additionally, 48.84 wt% biochar was obtained, offering both energy and active carbon.

A few studies have also been conducted on co-pyrolysis of these weed species with the waste polymeric substance. Radhaboy and Pugazhvadivu [2] conducted pyrolysis of *Calotropis procera* stem (CPS) and subsequently co-pyrolyzed CPS with waste polystyrene (WPS) in a 50:50 weight ratio in a fixed bed reactor at 500°C. This resulted in bio-oil yields of 6.28% for CPS and 47.34% for CPS-WPS co-pyrolysis. GC-MS analysis indicated that CPS bio-oil primarily consisted of phenolic compounds along with a few oxygenated, aliphatic, and cyclic compounds. In contrast, CPS-WPS bio-oil contained mono-aromatics, esters, and nitrogenated compounds. Co-pyrolysis resulted in bio-oil with reduced phenolic compounds and increased ester content.

This literature review underscores the potential of utilizing bio-wastes to produce third-generation biofuels and chemicals. The pyrolytic transformation of these resources offers a sustainable and viable approach to waste management. Converting bio-wastes, such as invasive weed species, through thermo-chemical processes not only addresses weed control in agriculture but also contributes to energy and chemical recovery. Furthermore, the solid char generated serves various functions, including enhancing soil

quality, rehabilitating polluted environments, and storing carbon, as mentioned in Chapter 1.

2.6 Catalytic Pyrolysis of Biomass

In the Introduction chapter, the potential applications of biomass pyrolytic liquid, also known as bio-oil, were discussed, which can be served as an energy carrier, a source for various commodity chemicals, or be upgraded to be used as a transportation fuel. However, the effective utilization of bio-oil as a viable alternative to petroleum fuels is hindered by several inherent drawbacks, including high acidity, density, viscosity, oxygen content, instability, immiscibility, water and oxygen content, and a relatively lower heating value compared to petroleum fuels [146-149]. Therefore, the improvement of bio-oil quality is imperative, involving the removal of undesirable components or their conversion into more desirable ones. Two primary methods employed for bio-oil upgrading are hydrotreating and catalytic cracking. In addition to these, steam reforming and esterification, etc can also be employed for upgradation of bio-oil. The use of hydrotreating, although effective, is limited by economic considerations due to the requirement for hydrogen input, high pressure, and catalyst deactivation issues [150, 151]. On the other hand, catalytic pyrolysis can be carried out at atmospheric pressure, with the choice of catalyst dependent on the desired end products [150, 152]. The catalytic pyrolysis can be categorized into two distinct processes based on the catalyst's placement within the reactor: (a) in-situ and (b) ex-situ. In the ex-situ catalytic pyrolysis process, pyrolytic vapors generated through the thermal breakdown of biomass pass through a separate catalytic bed, where they undergo further transformations into volatile organics, gases, and coke. In contrast, the in-situ catalytic pyrolysis process involves bringing the biomass feedstock and catalyst into direct contact by mixing them before initiating the pyrolysis process. The ex-situ process is generally associated with higher amounts of water and coke production compared to the in-situ process, which can result in a reduction in the liquid product yield. This is due to the extended residence time of pyrolytic vapors in the catalytic bed, leading to additional secondary reactions and coke formation. However, the primary advantage of the ex-situ process lies in its ability to independently control pyrolysis and catalytic temperatures. This independent control enhances the distribution of product components by allowing optimization of conditions in each stage of the process [130]. In comparison, in-situ catalytic pyrolysis involves simultaneous

interaction between biomass and catalyst, offering advantages in terms of direct catalyst-biomass contact and potential control over reaction pathways. It is important to note that the choice between in-situ and ex-situ catalytic pyrolysis depends on specific process goals, biomass characteristics, and desired product outcomes. Each approach has its advantages and challenges, and the selection should be based on optimizing the overall performance and efficiency of the pyrolysis process.

Catalytic pyrolysis, achieved through meticulous catalyst selection, aims to improve bio-oil yield and quality by diminishing acidity, viscosity, and oxygen content, and enhancing heating value. Simultaneously, it generates low-carbon chain compounds. In catalytic pyrolysis, the primary goal is to deoxygenate and convert the heavy oxygenated volatiles from biomass decomposition into lighter fuels and chemicals by engaging with an appropriate catalyst. Biomass catalytic pyrolysis presents numerous benefits, including the direct production of selective renewable hydrocarbons such as benzene, toluene, and xylene. Furthermore, all essential chemical reactions occur within a singular reactor. This method facilitates the production of liquid aromatics and olefins that seamlessly integrate with existing infrastructure [128].

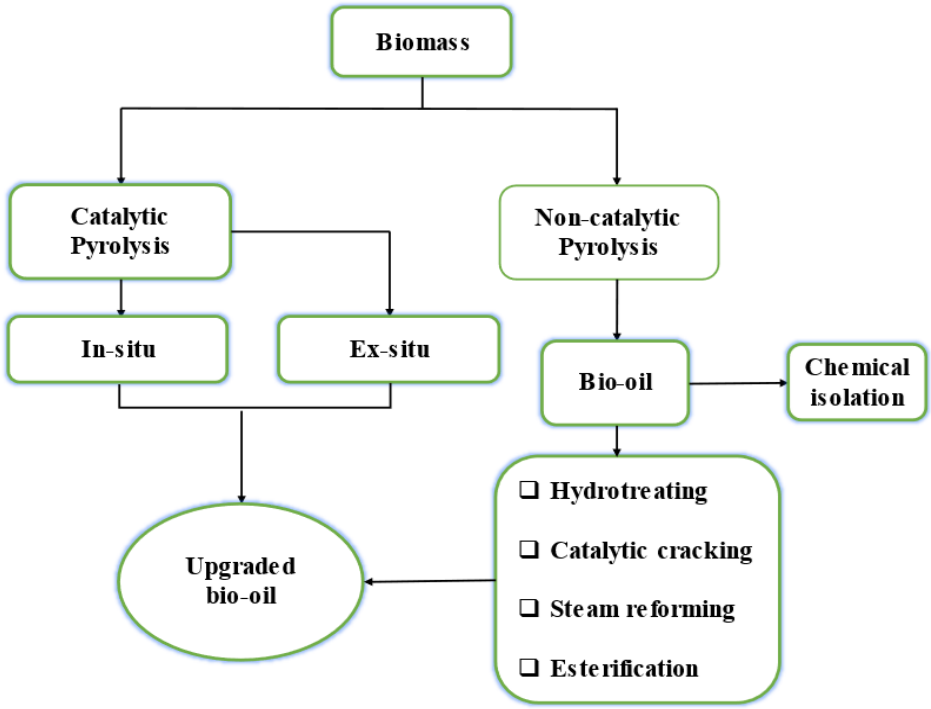

Fig. 2.1: Catalytic upgrading of biomass

The application of heterogeneous catalysts in biomass pyrolysis draws inspiration from the petrochemical industry, where they are extensively employed to convert heavy

oil fractions into lighter fuels and chemicals [235]. An ideal catalyst for biomass pyrolysis should yield high-quality bio-oil with minimal oxygen and water content while simultaneously minimizing the presence of undesirable compounds such as acids, ketones, and carbonyls [236]. Furthermore, the catalyst should demonstrate resistance to deactivation and maintain thermal stability. Reducing the oxygenated components in bio-oil can enhance its heating value and result in improved physical and chemical properties. Oxygen is eliminated from pyrolysis vapours in the form of CO_2, CO, and H_2O. Removing oxygen as CO_2 or CO is more favourable than H_2O to preserve hydrogen for hydrocarbon-forming reactions. CO_2-based oxygen removal effectively enhances the H–C ratio, thus reducing coke deposition.

Numerous research groups have shown significant interest in enhancing bio-oil quality through heterogeneous catalysis. The main challenges in advancing this technology pertain to the processing of lignocellulosic materials and the development and optimization of advanced porous materials serving as efficient monofunctional and bifunctional catalysts for producing transportation fuels from biomass.

2.6.1 Chemical Reactions in Catalytic Pyrolysis

The chemistry underpinning catalytic pyrolysis encompasses the examination of reaction mechanisms, the catalyst's function, and the impact of process conditions on bio-oil yield and quality. Numerous catalytic materials, including zeolites, mesoporous materials with uniform pore size distribution (such as MCM-41, MSU, and SBA-15), microporous or mesoporous hybrids infused with noble and transition metals, and base catalysts with bifunctional properties, have been explored as potential catalysts for biomass pyrolysis. This literature review offers a brief insight into the chemistry of catalytic pyrolysis and its potential for producing deoxygenated bio-oil. The pioneering work in the field of biomass feedstock conversion using zeolite catalysts was carried out by researchers at Mobil, who demonstrated that ZSM-5 could convert biomass feedstocks into hydrocarbons [129]. Catalytic biomass pyrolysis using molecular sieves primarily focuses on the generation of aromatic hydrocarbons. These hydrocarbons are highly sought after due to their elevated octane ratings and their applicability as octane boosters in gasoline. Furthermore, aromatic compounds serve as valuable precursors for various high-end chemicals and polymers [131]. Bridgewater, [132] underscores the pivotal role of aromatization in hydrocarbon reactions over zeolites, while Huber and Corma, [133]

propose that this aromatization process may proceed through a Diels-Alder reaction, in which olefins formed during thermal biomass cracking combine to create cyclic and aromatic compounds. However, achieving selective aromatics production hinges on minimizing the formation of undesired coke within the catalyst, as coke formation can lead to catalyst deactivation. Coke can originate from various sources, including biomass feedstock, volatile oxygenates, dehydrated species, or aromatics through homogeneous gas phase thermal decomposition reactions, as well as from heterogeneous reactions occurring on the catalyst [129].

As mentioned earlier, the pyrolysis process commences with the thermal decomposition of biomass, resulting in the formation of volatile organic compounds, gaseous products, and solid char. In the presence of catalysts, these organic volatiles undergo dehydration reactions, yielding water and dehydrated species. The dehydrated species subsequently infiltrate the pores of a zeolite catalyst, where they undergo a series of transformations leading to the production of aromatics, carbon monoxide (CO), carbon dioxide (CO_2), water, and additional coke. These transformations involve reactions such as cracking, decarbonylation, aldol condensation, decarboxylation, ketonization, isomerization, oligomerization, hydrodeoxygenation, hydrogenation, re-polymerization, and aromatization [175]. However, understanding the mechanisms of catalytic pyrolysis remains a challenge due to several factors. These include the complex reaction pathways influenced by the specific catalyst system and the diverse composition of biomass feedstock. Additionally, the intricate structure of the biomass matrix, limitations in mass transfer phenomena within the system, and potential catalyst immobilization further complicate the process [175, 178].

2.6.2 Factors Affecting Biomass Catalytic Pyrolysis

Zeolite catalysts have received much attention due to its relatively low cost, availability, and its potential to yield high quality bio-oil [175]. Extensive research has been conducted on employing traditional zeolites for enhancing bio-oil, but their utilization has been limited due to issues like coke deposition, low liquid yield, and the generation of polycyclic aromatic hydrocarbons [153, 154]. Similarly, mesoporous catalysts have been explored for bio-oil improvement, but their adoption has been constrained by inadequate hydrothermal stability and high production costs. However, efforts have been made to boost the production of aromatic compounds in the bio-oil

upgrading process using molecular sieves catalysts like HZSM-5, ZSM-5, MCM-41, SBA-15, HUSY, and their modified counterparts with varying porous structures. These catalysts facilitate the conversion of biomass pyrolysis vapors/oil into olefins and aromatics, which are fundamental components in the petrochemical industry. Amongst different zeolite catalysts, ZSM-5 (exhibiting high acidity and pore size) demonstrated excellent efficiency for bio-oil upgrading, producing less viscous, less acid, and high energy value bio-oil [179]. ZSM-5 also increased the concentration of aromatic hydrocarbons, organics, and gaseous compounds in bio-oil caused by aromatization, decarbonization, and cracking reactions [151, 175, 180]. The distribution of catalytically enhanced bio-oil hinges on several pivotal factors: characteristics of catalysts including porosity and acidity of catalyst, catalyst surface area, catalyst-to-biomass ratio, impregnation of metal into catalysts framework, etc.

2.6.2.1 Characteristics of catalysts

Porosity and acidity are two critical factors affecting the conversion of oxygenated biomass products into aromatics using catalysts. A study by Jae et al. [134] explored the impact of zeolite pore size and shape selectivity on the conversion of glucose to aromatics. The study revealed that the yield of aromatics was closely linked to the catalyst's pore size. Zeolites with smaller-pores were found to predominantly produce oxygenated products, CO, CO_2, and coke during glucose pyrolysis, with no significant aromatics production. In contrast, medium-pore zeolites (with pore sizes ranging from 4 to 5.5 Å). yielded the highest amounts of aromatics. On the other hand, zeolites with larger pores, such as SSZ-55, Beta zeolite, and Y-zeolite, resulted in higher coke formation, lower aromatic yields, and reduced oxygenate production, indicating that larger pores favour coke formation. Besides pore size, the internal pore space (i.e., pore intersections) and steric hindrance also play significant roles in aromatic production during pyrolysis. Zeolites with medium-sized pores, offering moderate internal pore space and steric hindrance (e.g., ZSM-5 and ZSM-11), exhibited the highest aromatic production and the lowest coke formation. In the catalytic pyrolysis of empty palm fruit bunches using Al-MCM-41 and HZSM-5, it was observed that Al-MCM-41 generated a higher quantity of phenols compared to HZSM-5 [137]. This difference can be attributed to the greater porosity of Al-MCM-41, which encourages phenol production. The catalytic activity is directly related to the structural and active site characteristics of the catalyst [138]. In a

study by Ma et al. [139], a comparison was made between the aromatic yields obtained through non-catalytic and catalytic pyrolysis of lignin using a porous catalyst silicate and HZSM-5. In non-catalytic pyrolysis, coke formation was the predominant outcome. However, the use of a porous catalyst without acid sites (silicate) resulted in the adsorption and stabilization of intermediates, forming compounds like phenol alkoxy and aromatic hydrocarbon alkoxy. This stabilization prevented re-polymerization reactions and led to reduced coke formation and higher liquid yield.

In addition to porosity, the presence of acid sites is essential in a catalyst to achieve a high yield of aromatics. Lignin is a particularly intriguing compound to study as a model for biomass catalytic pyrolysis. Despite being the most challenging biomass component to decompose, resulting in the highest production of solid residue [140-142], pyrolytic lignin has significant theoretical potential for conversion into aromatics [143]. In the catalytic cracking of lignin extracted from rice husks, catalyst activity followed the order of ZSM-5 > HZSM-5 > MCM-41 ~ SBA-15 > Beta, based on higher liquid production and reduced coke formation [143]. It was also noted that the formation of aromatics decreased in the order of ZSM-5 > HZSM-5 ~ Beta > MCM-41 > SBA-15, suggesting that microporous zeolites favor greater aromatic production. Phenols were significantly deoxygenated and converted into aromatics such as toluene, naphthalene, and benzene, with toluene, naphthalene, and benzene being the most abundant aromatic species produced over the ZSM-5 catalyst. Moreover, an increased concentration of polyaromatic hydrocarbons, including naphthalene, phenanthrene, fluorene, and their alkylated variants, in catalytically upgraded bio-oil was observed by Williams and Horne [136]. Some of these compounds are known carcinogens and/or mutagens, representing potential health hazards.

In addition to the above-mentioned influencing factors, the surface area of the catalyst also plays a significant role in determining product distribution and selectivity. A systematic and comprehensive study conducted by Lapps et al. [161] examined the impact of catalyst surface area in biomass pyrolysis. The study revealed that the more active the catalyst, meaning the higher the surface area, the less liquid was produced. However, the effect of the catalyst on bio-oil yield was not linear. The effect of the total surface area on gas yield was found to be logarithmic. Consequently, when using a less active catalyst, gas yield increased significantly compared to using zero surface area silica sand. However, further use of a higher surface area catalyst had a minor effect on gas yield. The

total surface area of the catalyst had a dominant effect on char yield, with char yield doubling when the highest activity catalyst was used.

Overall, the properties of catalysts such as porosity, acidity, surface area, etc. can affect the yield and quality of pyrolysis products, as well as the formation of coke and other byproducts. Catalysts with suitable porosity and acidity can help optimize the process and improve the efficiency of biomass pyrolysis.

2.6.2.2 Biomass to catalyst ratio

In addition to the parameters mentioned earlier, the ratio of catalyst to biomass is a crucial factor affecting both product formation and selectivity in biomass catalytic pyrolysis. Carlson et al. [129] demonstrated that product selectivity in catalytic fast pyrolysis of glucose with ZSM-5 is influenced by the catalyst-to-glucose weight ratio. As the catalyst-to-glucose ratio decreases, the coke yield increases, while the aromatic yield decreases. These thermally stable oxygenates act as intermediates in aromatic production and are formed more as the catalyst-to-glucose ratio decreases. In an another study by Zhao et al. [158], an increased catalyst-to-feed ratio led to a rise in aromatic hydrocarbon yield from 54.32% to 56.71%. Du et al. [159] investigated the same parameter in the catalytic pyrolysis of microalgae Chlorella. They observed a significant increase in aromatics yield as the catalyst-to-feed ratio increased from 1:1 to 5:1.

Ma et al. in 2020 [171] studied the impact of commercial zeolite catalysts on *Ulva prolifera* macroalgae pyrolysis for bio-oil yield and composition. They used catalysts like ZSM-5, Mordenite, and Y-Zeolite and applied biomass-to-catalyst ratios of 10:0.2, 10:0.5, and 10:1 at temperatures of 300, 350, 400, and 450 °C with a heating rate of 20 °C/min. For the ZSM-5 catalyst, the highest bio-oil yield (37.4 wt%) was obtained with 0.5 g of catalyst.

Rahman et al. [172] in 2020 investigated the effects of catalyst and biomass-to-catalyst ratio on the high yield of aromatic hydrocarbons. They explained how acidic and basic metal catalysts (i.e., ZSM-5 and CaO) influenced the yield of aromatic hydrocarbons from pinewood using Py-GC/MS to identify the chemical compounds in pyrolytic vapors. The highest aromatic yield of 42.19 wt% was reported for a biomass-to-ZSM-5 catalyst ratio of 0.25:1. On the other hand, no aromatics were detected for CaO, while a higher yield of phenolics (51.02 wt%) and a lower acidic fraction (1.35 wt%) were observed at the ratio of 0.25:1 (pinewood: CaO). ZSM-5 proved to be an effective

catalyst for aromatic hydrocarbons, while CaO showed the potential to reduce acidic fractions by facilitating acid deoxygenation into ketones.

2.6.2.3 Incorporation of metal to catalyst

In recent time, research on bifunctional catalysts, such as zeolites doped with noble metals, has been gaining popularity. The distribution of acid sites' strength on molecular sieve catalysts plays a crucial role in determining product distribution, and selectivity during biomass catalytic pyrolysis. This essential factor can be optimized by introducing metals into the catalyst. The incorporation of metals into the catalyst can influence both the formation of aromatics and olefins in catalytic biomass pyrolysis [175].

Iliopoulou et al. [162] noted that impregnating transition metals, such as nickel and cobalt, into ZSM-5 catalysts increased the production of aromatics from biomass feedstock. This effect was attributed to the transition metals promoting dehydrogenation reactions. Again, in an another study during the catalytic pyrolysis of pine wood in a pyro-probe reactor under hydrogen pressure, 5 wt.% impregnated Mo/ZSM-5 catalyst increased aromatics yield with increasing pressure. The production of aromatics from Mo/ZSM-5 was lower than HZSM-5 below 300 psi pressure, likely due to the reduction of zeolite acid sites occupied by Mo. However, at 400 psi, Mo-ZSM-5 led to higher aromatics production, as the promotion of hydrogenation reactions caused by Mo outweighed the reduction of zeolite acid sites [168].

The incorporation of metals into the catalyst can alter the operational conditions for product selectivity in biomass catalytic pyrolysis. In an investigation, Gong et al. [163] used a lanthanum-modified HZSM-5 catalyst in catalytic cracking of bio-oil and observed that adding lanthanum to the zeolite efficiently adjusted the acid distribution among strong, medium, and weak acid sites. This high percentage of medium acid sites was found to be suitable for selectively producing light olefins.

In the catalytic cracking of fast pyrolysis vapors of poplar wood using a Palladium (Pd) supported SBA-15 catalyst, it was found that the catalytic capabilities of the Pd/SBA-15 catalyst improved with an increase in Pd content from 0.79 wt.% to 3.01 wt.% [165]. Huang et al. [164] studied the catalytic conversion of various biomass feedstocks into olefins using HZSM-5 impregnated with 6 wt.% lanthanum. They observed that feedstocks with higher cellulose or hemicellulose content produced more olefins than

those with higher lignin content. Increasing the percentage of lanthanum from 2.9 to 6.0 wt.% enhanced olefin production from rice husk by 15.6% to 26.5%, respectively.

Cheng et al. [166] investigated the catalytic pyrolysis of biomass model compound (Furan) using Ga-ZSM-5 bifunctional catalyst to increase aromatic yield. They found that Ga species promoted decarbonylation and olefin aromatization reactions, while ZSM-5 was involved in oligomerization and cracking reactions. As a result, Ga-ZSM-5 yielded 15-23% more aromatics than HZSM-5 catalyst. The Ga species increased the rate of aromatic production without altering the overall reaction mechanism.

In a study by Du et al. [167], the effect of metal incorporation (Co, Cu, Fe, Ga, Mo, and Ni) on H-ZSM-5 on the aromatic yields of *Chlorella* and egg whites was examined. Among the catalysts, Cu and Ga significantly enhanced aromatics yields, indicating that certain transition metals can promote the aromatization function of HZSM-5.

Veses et al. [169] explored the impact of different metals (Mg, Ni, Cu, Ga, and Sn) impregnated in ZSM-5 zeolites on the properties of a catalytically upgraded organic phase of bio-oil from the pyrolysis of woody biomass. They observed significant improvements in the liquid's properties, such as lower viscosity and oxygen content, higher heating value, reduced acidic compounds, and an increased aromatic fraction when using catalysts. Among all the catalysts tested, Ni-ZSM-5 and Sn-ZSM-5 showed promise for catalytic upgrading of pyrolysis bio-oil.

Vichaphund et al. [170] investigated the influences of transition metals (Co, Ni, Mo, Ga, and Pd) incorporated into HZSM-5 during the catalytic fast pyrolysis of *Jatropha* waste. The addition of metals, including the catalysts, improved hydrocarbon production, particularly aromatics, and reduced oxygenated and nitrogen-containing compounds. Metal/HZSM-5 catalysts exhibited high selectivity for benzene, toluene, xylene, and relatively low naphthalene selectivity.

Overall, these studies highlight the significant impact of metal impregnation into catalysts on product selectivity and yield in biomass catalytic pyrolysis.

2.7 Exploring the Pyrolysis Kinetics through Thermogravimetric Analysis (TGA)

Thermogravimetric analysis (TGA) has proved to be a useful tool for elucidating the decomposition of various biomass materials. The temperature domains indicate the decomposition of various components present in biomass, and it is proven that each kind

of biomass has unique pyrolysis characteristics due to the specific proportions of the components [118]. Kinetic study of biomass pyrolysis becomes useful for a better understanding of the physicochemical process and proper design of industrial pyrolysis units. Usually, two methods are highlighted in literature viz. model-fitting as well as model-free methods to determine the kinetic parameters [119]. However, model-free methods are considered to be more suitable due to the absence of some drawbacks that are associated with model-fitting techniques. Model-free methods are based on the principle that, at constant conversion, the reaction rate depends only on temperature. Isoconversional methods are also model-free methods and using these methods it is possible to determine the apparent activation energy without evaluating the reaction model [182]. At the beginning of the century, the International Thermal Analysis and Calorimetry Society (ICTAC) showed that using a single scan rate method to process thermal analysis kinetic data gives results that are not reliable and cannot reflect the complex nature of a solid-state reaction [121]. As a result, the international thermal analysis community has called for the use of multiple scan rate methods to determine thermal analysis data. In addition, as a way to determine the complex nature of the reaction, it is necessary to determine the change in activation energy with conversion using the iso-conversion method [122]. The isoconversional approach is the more commonly adopted of the two main model-free methods and is increasingly being adopted in biomass thermochemical conversion research [123]. Isoconversional methods have the potential to estimate the behaviour of complex reactions; they are simple in nature; and they minimize the risks of selecting an unsuitable kinetic model and finding the wrong kinetic parameters [121]. Isoconversional methods have been widely used to examine the non-isothermal kinetic parameters of solid feedstocks in the pyrolysis processes [121], and they represent the most effective way with which to process thermogravimetric analysis (TGA) data in order to calculate effective activation energies for biomass pyrolysis [119]. In addition, isoconversional methods constitute an interesting and easy-to-use solution for the estimation of kinetic parameters, providing rather accurate results in the case of a one-step reaction, with errors lower than 1% [121]. All isoconversional methods are based on the principle that the reaction rate at a constant conversion degree is only a function of temperature [124].

As reported by Basu [176] pyrolysis process is composed of three stages drying, devolatilization, and carbonization. The study showed that drying or dehydration occurs within a temperature range of 30–150 ºC. Devolatilization occurs due to the release of

volatiles from the decomposition of hemicellulose and cellulose contents between 150 ºC and 400 ºC. According to Vassilev et al. [177], cellulose is a long network of hydrogen bonds that establishes a link between the long chains to provide thermal stability and resistance. The cellulose devolatilization temperature is between 250–350 ºC. Carbonization and char formation occur at above 400 ºC. According to Pasangulapati et al. [237], lignin is the higher precursor of char, with about 50% yield, whereas the contribution of cellulose and hemicellulose is very low, with 1% for cellulose and 7% for hemicellulose.

2.7.1 Pyrolysis Kinetics, Reaction Mechanism, and Thermodynamics Studies of Biomass

Numerous studies have explored the kinetics of biomass pyrolysis in different feedstocks, providing valuable insights into the activation energy, reaction mechanisms, and key parameters governing the pyrolysis process. For instance, studies on biochemical components like cellulose, lignins, or biomass such as olive kernel, corn stover, brown algae, cellulose, oil shale, elephant grass, *Typha latifolia, Mesua ferrea* tree, sawmill dust, etc. have shed light on the diverse kinetic behaviors in these materials. Researchers have employed a range of methods, such as isoconversional, non-linear, and model-fitting approaches, to investigate this kinetics. The findings highlight the importance of understanding the pyrolysis kinetics in diverse biomass materials and offer valuable insights for the design and optimization of thermochemical biomass conversion processes.

Saikia et al. [216] investigated the kinetic behavior of the biomass using Friedman, KAS, and FWO methods at various heating rates (10, 20, 40, and 60 °C/min). They determined an average activation energy of 151.45 kJ/mol, which was subsequently employed to evaluate the reaction mechanism via the Criado master plot

Jeguirim and Trouvé [195], examined the thermal behavior of *Arundo donax* using thermogravimetric analysis under an inert atmosphere. The heating rates used ranged from 5 to 20 °C/min, covering a temperature range from room temperature to 750 °C. The thermal degradation process of *Arundo donax* was found to manifest in two distinct phases. The initial phase, known as the “active zone”, primarily involves the breakdown of hemicellulose and cellulose polymers. This phase commenced at a relatively low temperature of 200 °C when compared to traditional wood samples and concluded at 350

°C. The subsequent phase, named the “passive zone”, encompassed the pyrolysis of the lignin polymer and occurred between 350 and 750 °C. During the active zone, carbon oxides were released, while the passive zone primarily led to the formation of volatile organic compounds (VOCs). Variations in heating rates significantly impacted mass losses, mass loss rates, and emission factors within the active zone. The study revealed that the overall pyrolysis of *A. donax* could be accurately characterized using a global independent reactions model for hemicellulose and cellulose in the active zone. The activation energy for hemicellulose remained relatively constant, approximately 110 kJ/mol, even with changes in heating rates, and exhibited a reaction order of around 0.5. On the other hand, an increase in heating rate was associated with a decrease in the activation energy for cellulose, although a first-order reaction was observed for cellulose decomposition.

Li et al. [196] explored the pyrolytic characteristics and kinetics of two brown algae, *Laminaria japonica* and *Sargassum pallidum*. Their experiments carried out in an inert atmosphere at various heating rates, revealed three stages: moisture evaporation, primary devolatilization, and residual decomposition. Significant differences were observed in average activation energy, thermal stability, final residuals, and reaction rates between the biomass samples. The activation energies for *L. japonica* and *S. pallidum* were 207.7 and 202.9 kJ/mol, respectively. The reaction mechanism followed by *L. japonica* and *S. pallidum* was Avrami–Erofeev function (n = 3).

In 2013, Sanchez-Jimenez and coworkers [199] investigated the kinetics of cellulose pyrolysis using various heating schedules, including linear heating rate, isothermal, and constant rate thermal analysis (CRTA). They applied isoconversional and master plot methods to identify the kinetic model governing the reaction. Their results indicated an activation energy of 191 kJ/mol and a kinetics mechanism governed by a chain scission reaction. The analysis provided accurate and consistent results without assuming a specific kinetic model, reducing the risk of inappropriate model fitting.

In 2013, Chutia et al. [197], the physicochemical properties of *Mesua ferrea* deoiled cake (MFDC) were explored, and the pyrolytic characteristics and kinetics of MFDC were assessed using TGA at three different heating rates (10, 20, and 40 °C/min). They applied various kinetic models, including Arrhenius, Coats-Redfern, Flynn-Wall Ozawa (FWO), and the Global Independent Reactions model. The average activation energies were determined to be 43.77-54.12 kJ/mol for active pyrolysis zone-1 (SII) and

146.98- 256.82 kJ/mol for active pyrolysis zone-2 (SIII). The reaction order for the feedstock was found to be 0.97.

Mishra et al. [202] investigated model-free kinetic of pinewood pyrolysis in 2015, using a TGA analyzer in an inert atmosphere. Non-isothermal model-free kinetic methods were employed at six different heating rates (5–40 ºC/min). The study revealed three distinct zones in the isoconversional plot. Average activation energies of 134.32 kJ/mol, 146.89 kJ/mol, and 155.76 kJ/mol were determined for conversion ranges of 1–22%, 24–84%, and 85–90%, respectively, in zones I, II, and III. The decomposition mechanism followed a diffusion mechanism up to a conversion value of 0.7, after which it transitioned to a 1½ order reaction. Both methods fit a 2D diffusion mechanism well across a wide range of conversions, and the isoconversional analysis was validated by close agreement with isothermal predictions at 400 °C.

Collazzo et al. [204] conducted a comprehensive non-isothermal kinetic investigation of elephant grass at various heating rates (5–50 K/min) spanning temperatures from 473 to 773 K. Activation energy was assessed using both model-free (Isoconversional KAS and FWO) and non-linear (Vyazovkin advanced isoconversional) methods. The results indicated a relatively consistent activation energy up to a conversion of 0.6, with an average of 185.28 ± 6.87 kJ/mol using Vyazovkin advanced isoconversional methods. The decomposition mechanism was characterized by two successive reactions: diffusion followed by a reaction-order model. Activation energy values ranged from 46.5 to 65.5 kJ/mol for hemicellulose, 108.0 to 127.2 kJ/mol for cellulose, and 45.6 to 53.5 kJ/mol for lignin. These findings have potential applications in bench or pilot-scale thermochemical biomass conversion processes.

Ahmad et al., [208] evaluated the kinetics, thermodynamic parameters, and pyrolysis reaction mechanism for *Typha latifolia* using thermogravimetric analysis and artificial neural networks (ANN). They employed Flynn-Wall-Ozawa (FWO), Kissinger-Akahira-Sunose (KAS), and Coats-Redfern methods to describe the reaction mechanism, encompassing order-based reactions, diffusion, and contracting geometry. The average activation energy values, determined by both KAS and FWO methods, were approximately 184 kJ/mol and 182 kJ/mol. Furthermore, the analysis revealed the pyrolysis process as having two distinct regions: Region-I ($0.1 \leq \alpha \leq 0.4$) characterized by diffusion, and Region-II ($0.4 \leq \alpha \leq 0.8$) dominated by order-based reactions.

In Gogoi et al. investigation [205], they studied the pyrolysis kinetics and mechanisms of *Mesua ferrea* tree and sawmill dust using thermogravimetric methods.

They explored a temperature range of 30–800 °C with heating rates of 5, 10, and 20 °C/min. Activation energies were calculated using differential and integral isoconversional methods, including the Friedman method, KAS method, FWO method, and Tang method. The apparent activation energies for both biomass types fell within the range of 180–380 kJ/mol. These values were dependent on fractional conversions and the non-parallel nature of Friedman plots, which supported the results obtained from the master plot method. The Z(α) master plot method indicated that the initial thermal decompositions of both biomass types followed nucleation models, transitioning to three-dimensional diffusion models. Arrhenius constants derived from Friedman activation energy values ranged from 1.74×10^{18} to 5.78×10^{23} min^{-1} for *Mesua ferrea* tree and 1.61×10^{20} to 5.31×10^{23} min^{-1} for sawdust. This study demonstrated the potential of using a combination of FWO or KAS methods with the Friedman method to calculate apparent activation energies of biomass residues more effectively.

Arenas et al. [121] studied the kinetics and mechanism of pyrolysis for various materials, including pineapple, orange, and mango peel wastes, agro-industrial by-products, rice husk, and pine wood, were analyzed using five isoconversional methods (KAS, FWO, Starink, Vyazovkin, and Friedman) and one model-fitting method (DAEM). Activation energy patterns were similar across all six methods. Notably, fluctuating activation energy levels were observed for fruit peel wastes in the entire conversion range (150–550 kJ/mol), while agro-industrial by-products exhibited a stable profile (180 kJ/mol) up to 80% conversion. These fluctuations and the high number of reactions were associated with the high extractive content in the peel samples (approximately 30 wt %).

Sahoo et al. [107] evaluated the kinetics of thermal decomposition for *Prosopis juliflora* (PJ) and *Lantana camara* (LC) using thermogravimetric analysis. The kinetic and thermodynamic parameters of the pyrolysis process were determined under four heating rates (5, 10, 20, and 40 °C/min) through Non-linear integral (NL-INT), non-linear differential (NL-DIF), and model-free (M-FRM) methods. The average activation energy (Ea) values were found to be in the range of 140-157 kJ/mol for PJ and 149-170 kJ/mol for LC, depending on the method. The overall pyrolysis process for PJ and LC followed order-based models (F_n) and diffusional models (D_n). The thermodynamic parameters ΔH and ΔS indicated positive and negative values, respectively, suggesting non-spontaneous reactions at all temperatures.

Pandey et al. [238] in 2021 investigated the pyrolysis kinetics of *Argemone mexicana* seeds, which are commonly found as naturalized weeds in agricultural fields.

They conducted thermogravimetric analysis under a nitrogen (N_2) atmosphere, subjecting the seeds to heating rates of 10°C/min, 20°C/min, and 30°C/min. To assess the kinetic parameters, including activation energy, pre-exponential factor, and thermodynamic properties, the researchers employed five kinetic methods: Kissinger–Akahira–Sunose (KAS), Ozawa-Flynn-Wall (OFW), Friedman (FRM), Starink (STR), and Vyazovkin (VYZ), as well as a model-fitting approach known as the Kennedy and Clarke method. The activation energies obtained from the KAS, OFW, FRM, STR, and VYZ methods were found to be 174 kJ/mol, 185.08 kJ/mol, 212.86 kJ/mol, 175.11 kJ/mol, and 174.36 kJ/mol, respectively. Additionally, the researchers identified an appropriate reaction mechanism using the master plot method. When using the Kissinger approach at different heating rates, the average pre-exponential factors were calculated to be 8.23×10^{22}, 1.68×10^{22}, and 8.05×10^{21} s^{-1}. At a lower heating rate of 10°C/min, the average values for the thermodynamic parameters (ΔH, ΔG, and ΔS) were determined to be 169.28 kJ/mol, 212.64 kJ/mol, and -70.95 J/mol. Their study suggests that the *Argemone mexicana* seeds have the potential to serve as a promising alternative source for biofuel production.

Ahmad et al. [223] also elucidate the pyrolysis reaction mechanism of desert plant *Calotropis procera,* pyrolyzed at four heating rates including 10 °$Cmin^{-1}$, 20 °$Cmin^{-1}$, 40 °$Cmin^{-1}$, and 80 °$Cmin^{-1}$. The pyrolysis reaction kinetics and thermodynamics parameters were assessed using isoconversional models namely Kissenger-Akahira-Sunose, Flynn-Wall-Ozawa, and Starink. Major pyrolysis reaction occurred between 200 and 450 °C at the conversion points (α) ranging from 0.2 to 0.6 while their corresponding reaction parameters including activation energy, enthalpy change, Gibb's free energy, and pre-exponential factors ranged from 165 to 207 kJ mol^{-1}, 169-200 kJ mol^{-1}, 90-42 kJ mol^{-1}, and 10^{18}-10^{26} s^{-1}, respectively. The narrow range of pre-exponential factors indicated uniform pyrolysis, while lower differences between enthalpy change and activation energies indicated that reactions were thermodynamically favorable.

2.7.2 Exploring the Kinetics and Thermodynamics in Catalytic Pyrolysis

The use of catalysts in biomass pyrolysis brings about changes in the kinetic parameters, thermodynamics, and reaction mechanisms of the pyrolysis process. However, there is a notable scarcity of literature addressing the kinetics and thermodynamics of catalytic biomass pyrolysis.

In a study by Xu et al. in 2017 [210], the pyrolysis kinetics and mechanisms of catalysts blended with *C. pyrenoidosa* algal biomass were investigated through thermal gravimetric analysis (TGA). Various catalysts, such as HZSM-5, rare earth metal impregnated ZSM-5 (Ce(I)/HZSM-5, Ce(II)/HZSM-5, La(I)/HZSM-5, La(II)/HZSM-5, and Pr-Nd/HZSM-5), were mixed into the biomass solution at a 5% biomass weight ratio. Kinetic analysis, based on the Arrhenius equation, revealed that all the metal-loaded HZSM-5 catalysts, except for La(II)/HZSM-5, improved their catalytic activity. Furthermore, the catalytic pyrolysis processes could be well described by first-order kinetic reactions, with Ce(I)/HZSM-5 exhibiting the lowest activation energy for catalytic pyrolysis of *C. pyrenoidosa.*

In 2018, Wang et al. [211] examined both the pyrolysis and catalytic pyrolysis behavior of Douglas fir (DF) using TGA. They developed kinetic models using Model-Free (Friedman) and Model-Fitting (Coats–Redfern) methods. DF and ZSM-5 were blended at a 1:3 mass ratio, and TGA was conducted within a temperature range of 25 to 600 °C with heating rates of 10, 20, 30, and 40 °C/min. Py-GC/MS was employed to analyze the chemical composition of the bio-oil product. The addition of a ZSM-5 catalyst slightly reduced the thermal degradation temperature of the biomass. ZSM-5 also significantly enhanced the production of aromatic hydrocarbons by reducing oxygen-containing compounds during DF pyrolysis. It led to an increased reaction rate and decreased energy requirements for the decomposition process. Notably, the activation energy calculated from Coats–Redfern and Friedman methods was higher for DF pyrolysis compared to catalytic pyrolysis.

Li et al. in 2020 [212] also investigated the influence of Lime mud (LM) as a CaO catalyst on the pyrolysis of herbaceous corncob (HC) and woody aspen sawdust (WS) was analyzed at a biomass-to-catalyst ratio of 1:1. Kinetic parameters were determined using the iso-conventional methods FWO and KAS, and the reaction order was calculated using the Avrami Theory. The catalyst was found to reduce the energy barrier of pyrolysis, and the variation interval of ΔH for HC and WS was significantly reduced by LM addition. However, ΔG was minimally affected by LM throughout the entire pyrolysis process.

2.8 Methodology for the Optimization of Process Parameters

Process parameter optimization in any process or methods aims to reduce the number of experiments, minimize time requirements, and cut costs. Traditional or classical optimization methods involve varying one parameter at a time while keeping others constant. Due to the length, large number of experiments, and failure to develop an understanding of the interaction effect; the classical or traditional approach has some disadvantages. In addition to that, the classical way is a time-consuming as well as expensive approach to attain optimum conditions. On the contrary, statistical optimization or mathematical modeling entails the simultaneous optimization of all parameters through a mathematical algorithmic process [191, 203, 206]-244]. This methodology is considered an important tool for gathering knowledge on the significance of the factors affecting pyrolyser performance. Generally, response surface methodology (RSM) and artificial neural network (ANN) are two statistical tools, which are employed for experimental design, statistical modelling and optimization of all the process parameters together [212, 213]. They enable us to predict and establish a relationship between one or more responses with independent factors [214, 215].

2.8.1 Response Surface Methodology (RSM)

Response Surface Methodology (RSM) was introduced by Box and colleagues [191] back in 1951, with its name originating from the graphical representation produced as a result of fitting a mathematical model. RSM is a suite of mathematical and statistical techniques employed for modelling and analyzing engineering or science problems in research. The primary goal of this methodology is to optimize an output variable (termed "response") that is influenced by several input variables (termed "independent variables"). This technique involves a series of experimental tests, known as "runs"; during which adjustments are made to the input variables in order to discern the factors responsible for changes in the output response. Numerical errors may arise due to factors like incomplete alignment of repeating processes, round-off errors, or differences in the representation of continuous physical phenomena [203].

RSM plays a pivotal role in developing a robust empirical model for gaining insights into the underlying mechanisms of any subject under study. It helps in minimizing the number of experimental trials needed to evaluate various parameters. It is also valuable for predicting the individual and interactive effects of various experimental

parameters. RSM blends statistical techniques with mathematical algorithms to address problems influenced by numerous potential factors and provides a more precise, insightful, and efficient approach to experimental design and optimization [203]. Optimization, in this context, refers to identifying the levels of independent variables that result in the maximum value of the output variable [203]. Furthermore, optimal designs are those constructed based on a certain criterion, often involving the "closeness" of the predicted response. Optimization serves to reduce the impact of noise. In multi-response experiments, the term "optimum" can sometimes be ambiguous, as there is no one-size-fits-all method for resolving the data. Conditions that are optimal for one response may differ from other responses or may even be physically impractical from an experimental standpoint. Subsequently, the response can be visually represented, either in three-dimensional space or as contour plots, aiding in the visualization of the shape of the response surface.

As bio-oil holds numerous applications, particularly as an alternative fuel source or for chemical recovery, researchers focused on enhancing both the quantity and quality of bio-oil yields from biomass pyrolysis. The high bio-oil yield hinges on several parameters, including temperature, particle size, heating rate, gas flow rate, etc. Determining the optimal conditions for bio-oil production entails testing the effects of various parameters on the pyrolysis process. Yet, the complexity arising from the combination of multiple parameters can make it challenging to identify the optimal combination through traditional experiments. In this context, a statistical experimental design approach such as Response Surface Methodology (RSM) has been applied to pinpoint the best parameter combination with the fewest experiments [125]. To date, there have been only a handful of studies focusing on the statistical optimization of experimental design using RSM in pyrolysis. Several notable examples are highlighted below:

Kilic et al. [126] conducted experiments to optimize the pyrolysis of *Euphorbia rigida* for bio-oil production, utilizing RSM based on a central composite design (CCD). The optimum conditions involved a reaction temperature of 600 ºC, a heating rate of 200 ºC/min, and a nitrogen flow rate of 100 mL/min, resulting in a maximum bio-oil yield of 35.3%.

Abnisa et al. [212] explored the pyrolysis of palm shell waste for bio-oil production and employed RSM based on CCD to determine the optimal conditions. The results, explained by a second-order polynomial equation, showed an optimal bio-oil

yield of 46.4 wt.% under the conditions of 500 ºC temperature, 2 L/min N_2 flow rate, 2 mm particle size, and 60 minutes of reaction time.

Isa et al. [127] employed a CCD design matrix in response surface methodology to determine the optimum pyrolysis conditions for rice husks. The optimal conditions were found to be a pyrolysis temperature of 473.37 ºC, a heating rate of 100 ºC/min, a particle size of 0.6 mm, and a holding time of 1 minute.

Jamaluddin et al. [231] reported the pyrolysis of palm kernel shells (PKS) using microwave-assisted pyrolysis. They used response surface methodology based on a central composite rotatable design (CCRD) to identify the predicted optimum conditions, resulting in calorific value, fixed carbon content, volatile matters content, and yield percentage of 29.9 MJ/kg, 59.8 wt%, 36.4 wt%, and 40.0 wt%, respectively.

Abnisa et al. [228] studied the co-pyrolysis of palm shells and polystyrene waste to obtain high-quality pyrolytic liquid. Using RSM, they determined that the maximum liquid yield, around 68.3%, was achieved at optimum conditions of a temperature of 600 ºC, a palm shell/polystyrene ratio of 40:60, and a reaction time of 45 minutes.

Jung et al. [230] performed fixed-bed reactor pyrolysis of lignin and used RSM to optimize operating variables. The maximum bio-oil yield of 30.1% was predicted and 29.3% was achieved under the optimum conditions: 669 ºC temperature, 15 ºC/min heating rate, and 6.97g loading mass. The bio-oil produced in these conditions contained a higher amount of 2-methoxyphenol.

Saikia et al., in 2018 [84], focused on the pyrolysis of perennial grass (*Saccharum ravannae L*) in a fixed bed reactor. By employing RSM based on CCD, they identified the optimal conditions: a temperature of around 550°C, a heating rate of around 20°C/min, and a nitrogen flow rate of around 226 mL/min, resulting in a maximum bio-oil yield of 39.8%. The experimental yield of 38.1% aligned well with the predicted value.

Tripathi et al., in 2020 [217], utilized microwave pyrolysis for oil palm shells to synthesize microporous and carbonaceous char. They applied Response Surface Methodology (RSM) to optimize operating parameters, resulting in a maximum char yield of 60.93% and a BET surface area of 250.03 m^2/g at the following conditions: Microwave power (MWP) of 1080.81 W, radiation time (RT) of 29.95 minutes, and nitrogen flow rate (NFR) of 133.48 cm3/min. Experimental results deviated only slightly from the predicted values, with a 6.75% deviation in OPS char yield and a 6.23% deviation in BET surface area.

In a recent investigation, Ilo et al. (2023) [227] placed a strong emphasis on utilizing the response surface methodology provided by Design-Expert to enhance the liquid fraction yield in the pyrolysis of a well-studied aquatic weed, water hyacinth by optimizing key process parameters, particularly temperature and particle size. Experiments were carried out across a temperature spectrum spanning from 273.22 to 676.78 °C, encompassing a range of particle sizes between 380 and 2620 μm, and maintaining a consistent heating rate of 30 °C/min along with a nitrogen flow rate of 25 l/min. The findings indicated that elevating the temperature and increasing the particle size resulted in a higher yield of the liquid fraction, while simultaneously reducing the char production. Specifically, the liquid fraction saw an increase from 24.36 wt.% at 273.22 °C to 48.45 wt.% at 575 °C and then decreased to 25.56 wt.% at 626.78 °C. Concurrently, char content decreased from 58.21 wt.% to 33.84 wt.% at 626.78 °C. Consequently, the researchers determined that the quadratic model was well-suited for the optimization of these variables. The statistical analysis of variance confirmed a strong alignment between the actual data and the model's predictions. This study argues that the valorization of water hyacinth if complemented by appropriate policies and strategic approaches, has the potential to generate a range of comprehensive socio-economic and environmental benefits. By identifying and implementing the optimal conditions for achieving an enhanced liquid fraction, the commercial potential of water hyacinth can be significantly influenced.

These studies collectively demonstrate the efficacy of RSM in optimizing pyrolysis processes for enhanced bio-oil yield and product quality. The insights derived from the above-mentioned literature will provide valuable input for policy discussions and the formulation of strategies aimed at leveraging the full potential of biomass.

2.8.2 Artificial Neural Network (ANN)

An artificial neural network (ANN) is a promising alternative modeling technique inspired by biological neural systems e.g., the brain [207]. It consists of a large number of neurons or processing elements or units in different layers that are interconnected to one another through weights. Through adjusting connecting weights, bias, and architecture; neurons are trained to perform a particular task [120]. The network architecture of neural networks was determined by how artificial neurons were mutually connected, and more than fifty types of network architecture could be found in the

literature [76]. The systems showing nonlinearities and complex behavior can be well predicted using neural networks due to their ability to learn from a set of experimental data (e.g., process conditions and responses) with minimal prior knowledge about their further properties and mechanisms.

A feedforward or backpropagation network is a widely used neural network consisting of several inputs and one output in each processing element [76]. A multilayer perceptron (MLP) is a feedforward ANN that is comprised of three or more layers of neurons. Independent input variables from the first layer of neurons (i.e. input layer) are connected to neurons of hidden layers. Propagation of the data from the input layer to the first hidden layer within the network occurred via the connections and the associated activation functions combined and modified those. Each layer has a certain number of neurons with corresponding weight and bias; and the ANN model for a particular task was dependent upon the nature of these connections, which provides additional adjustable parameters. In this way, the signals were propagated through each layer until they reached the output layer. The impact of each input neuron and its complex interactions can be identified by employing learning algorithms. Optimized ANNs are capable of approximating any continuous non-linear function, being highly resistant to missing or noisy data [207].

Both RSM and ANN are statistical tools that are employed for experimental design, statistical modelling, and optimization [213]. They enable us to predict and establish a relationship between one or more responses with independent factors [214, 215]. Out of these two, RSM is the most widely adopted statistical tool for the modelling and optimization of bio-oil yield in the pyrolysis process [182]. Although Neural Networks have been extensively used in many areas of prediction and modelling research in engineering and sciences [80, 84, 121, 207, 209], their use is limited in the pyrolysis process. Only a few research articles were dedicated to the application of ANN in the prediction of biochar yield or for the evaluation of kinetic parameters in the pyrolysis process [76, 80, 234]. But ANN can simply overcome the drawbacks of RSM due to its flexible nature and it is possible to build a trustable ANN model by allowing the addition of new experimental data. Also, ANN inherently captures almost any form of non-linearity [148]. There are no specific equations generated in the ANN model. However, ANN model generation involves a large number of iterative calculations, while the RSM model is calculated on a single step. Moreover, an ANN model can take a high computational time to construct and cost more than a response model. RSM is based on

mathematical relations for predicting the desired output, while ANN is based on algorithms which makes it more suitable for data fitting, modeling, and prediction [89, 93]. RSM is a verified technique used for the optimization and modelling of various processes at reasonable precision and accuracy with a lesser number of experiments that are adequate to obtain statistically acceptable results [83, 84]. RSM used regression equation to analyze the interaction factors and to identify the insignificant factors in the model and thus can reduce the intricacy of the problem [82]. However, the major drawback of RSM is that sometimes it is incapable of representing a given relationship at a desired level of accuracy.

Angın and Tiryaki in 2016 [81] employed both ANN and RSM to determine the mathematical correlation between temperature and heating rates of pyrolysis on the product yield of safflower seed press cake. They reported that ANN can be an alternative to RSM. However other than that there is no other established information on the comparative performance assessment of fixed bed-pyrolysis system on bio-oil yield using RSM and ANN. Therefore, to eradicate the knowledge gap due to the scarcity of the literature on the comparative analysis of both models attracts us to investigate the efficacy of both models for the prediction of bio-oil yield from a biomass sample taking more variables.

Aydinli et al., in their 2017 study [218], employed an Artificial Neural Network (ANN) model to predict the distribution of solid, liquid, and gas products in the pyrolysis process using various biomass components and process parameters as input. Specifically, they considered Cellulose, hemicelluloses, lignin, ash, fixed carbon, volatiles, moisture, and Pyrolysis temperature as input variables. With this approach, they successfully estimated the percentages of biomass pyrolysis products, including char, tar, and gas. Notably, this ANN model allowed for rapid predictions without the need for extensive experimental work.

Madhu et al., in their 2017 study [219], delved into the effects of pyrolysis parameters on the distribution of pyrolysis products in Flash pyrolysis and the characterization of bio-oil. They utilized the ANN methodology in conjunction with Rotatable Central Composite Design. In their model, they considered process parameters such as Temperature, Particle size, and sweep gas flow rate as inputs. The ANN model predicted that the maximum bio-oil yield, approximately 52.2 wt%, could be achieved under optimal conditions, which included a temperature of 450°C, a particle size of 0.8 mm, and a sweep gas flow rate of 1.75 m^3/h. Furthermore, their analysis revealed that

temperature had the most significant influence on the optimization process, surpassing the impact of particle size and sweep gas flow rate.

In the above-mentioned studies, Artificial Neural Network models served as powerful tools for predicting and optimizing the outcomes of pyrolysis processes, making it possible to streamline experimentation and gain valuable insights into the distribution of pyrolysis products and bio-oil characteristics. These models demonstrated their efficacy in providing quick and reliable results, ultimately contributing to the advancement of pyrolysis research and applications.

2.9 Summary of the Literature Review and Scope of Research

Pyrolysis garners attention for its potential to yield diverse products from a wide array of biomass feed stocks including invasive weed species, and there are a lot of weedy plants still available, the viability of which needs to be checked. *Tithonia diversifolia* is one such invasive plant and there is no prior literature regarding the thermochemical conversion of this weed species, despite its global abundance, making it a worthwhile candidate for pyrolytic valorization.

Recent literature highlights pyrolysis as a cost-effective, eco-friendly, and versatile method for converting different biomass into valuable products, and pyrolysis outcomes heavily depend on factors like feedstock, kinetics, reactor configuration, temperature, particle size, heating rate, residence time, and more. While the effects of process parameters, such as temperature, particle size, heating rate, and nitrogen flow rate, have been studied globally, they may vary from feedstock to feedstock. Also, there is a notable gap in knowledge concerning the comparative analysis of optimization methods like Response Surface Methodology (RSM) and Artificial Neural Networks (ANN) for predicting product yield in fixed bed pyrolysis processes. Investigating the effectiveness of both models in predicting product yield (such as bio-oil yield) from biomass while considering multiple process variables would contribute significantly to filling this knowledge void.

Although biomass pyrolytic liquid holds promise as an energy source and commodity chemical feedstock, it poses challenges as a low-grade fuel due to properties like corrosiveness, high density, acidity, water content, and instability. Consequently, bio-oil upgrading is imperative for transportation and commercial applications, necessitating catalytic upgrading. Several catalysts, including zeolites, exhibit potential in enhancing

bio-oil quality, albeit with a slight reduction in yields. Thus, research in biomass catalytic pyrolysis is vital for identifying optimal catalysts to improve downstream bio-oil upgrading processes, and ZSM-5 is one such catalyst on which there is a scarcity of studies on the use of ZSM-5 catalysts impregnated with transition metals for upgrading pyrolytic oil.

Understanding the kinetics and thermodynamics of biomass pyrolysis is also essential for process scaling, reactor design, and optimization. While significant research has explored biomass kinetics using model-free and model-fitting methods, only a limited number of investigations have been conducted to comprehend the pyrolysis kinetics of lignocellulosic biomass using the Combined Kinetics model, along with the Isoconversional methods. Bridging these knowledge gaps would enhance our understanding of biomass pyrolysis. It is imperative to conduct research that explores the interaction between pyrolysis kinetics, reaction mechanisms, and experimental pyrolytic studies of biomass when utilizing catalysts such as metal-impregnated ZSM-5.

References

1. Gent, S., Twedt, M., Gerometta, C., and Almberg, E. Introduction to Thermochemical Conversion Processes. Theoretical and Applied Aspects of Biomass Torrefaction, pages 1–16, 9780128095171, Butterworth-Heinemann, 2017. doi:10.1016/b978-0-12-809483-9.00001-4
2. Radhaboy, G., and Pugazhvadivu, M. (2020, March). Properties of Bio-Oil Produced by Co-Pyrolysis of *Calotropis procera* Stem and Waste Polystyrene. In *AIP Conference Proceedings*, Volume 2225, Number. 1. AIP Publishing.
3. Brownsort, P. A. Biomass pyrolysis processes: performance parameters and their influence on biochar system benefits. Master's Thesis, University of Edinburgh, 2009.
4. Venderbosch, R.H., Prins, W. Fast pyrolysis technology development. *Biofuels, Bioproducts and Biorefining*, 4 : 178–208, 2010.
5. Akhtar, J., and Amin, N. S. A review on operating parameters for optimum liquid oil yield in biomass pyrolysis. *Renewable and Sustainable Energy Reviews*, 16(7):5101-5109, 2012.
6. Kaur, R., Gera, P., and Jha, M. K. Study on effects of different operating parameters on the pyrolysis of biomass: A Review. *Journal of Biofuels and Bioenergy*, 1(2):135-147, 2015.

7. Kan, T., Strezov, V., and Evans, T. J. Lignocellulosic biomass pyrolysis: A review of product properties and effects of pyrolysis parameters. *Renewable and Sustainable Energy Reviews*, 57:1126-1140, 2016.
8. Fushimi, C., Araki, K., Yamaguchi, Y., and Tsutsumi, A. Effect of heating rate on steam gasification of biomass. 2. Thermogravimetric-mass spectrometric (TG-MS) analysis of gas evolution. *Industrial & Engineering Chemistry Research*, 42(17):3929-3936, 2003.
9. Antal, M. J., and Grønli, M. The art, science, and technology of charcoal production. *Industrial and Engineering Chemistry Research*, 42(8): 1619-1640, 2003.
10. Wang, S., Guo, X., Wang, K., and Luo, Z. Influence of the interaction of components on the pyrolysis behavior of biomass. *Journal of Analytical and Applied Pyrolysis*, *91*(1): 183-189, 2011.
11. Yang, Y., Li, T., Jin, S., Lin, Y., & Yang, H. (2011). Catalytic pyrolysis of tobacco rob: Kinetic study and fuel gas produced. *Bioresource Technology*, 102(23), 11027-11033.
12. Ball, R., McIntosh, A.C., & Brindley, J. Feedback processes in cellulose thermal decomposition: implications for fire-retarding strategies and treatments. *Combustion Theory and Modelling*, 8 (2), 281-291, 2004.
13. Burhenne, L., Messmer, J., Aicher, T., and Laborie, M. P. The effect of the biomass components lignin, cellulose and hemicellulose on TGA and fixed bed pyrolysis. *Journal of Analytical and Applied Pyrolysis*, *101*, 177-184: 2013.
14. Friedl, A., Padouvas, E., Rotter, H., and Varmuza, K. Prediction of heating values of biomass fuel from elemental composition. *Analytica Chimica Acta*, 544(1-2):191-198, 2005.
15. Fahmi, R., Bridgwater, A. V., Donnison, I., Yates, N., and Jones, J. M. The effect of lignin and inorganic species in biomass on pyrolysis oil yields, quality and stability. *Fuel*, 87(7):1230-1240, 2008.
16. Huang, Y. F., Kuan, W. H., Lo, S. L., and Lin, C. F. Hydrogen-rich fuel gas from rice straw via microwave-induced pyrolysis. *Bioresource Technology*, 101(6):1968- 1973, 2010.
17. Dominguez, A., Menéndez, J. A., and Pis, J. J. Hydrogen rich fuel gas production from the pyrolysis of wet sewage sludge at high temperature. *Journal of Analytical and Applied pyrolysis*, 77(2):127-132, 2006.

18. Janse, A. M. C., Westerhout, R. W. J., and Prins, W. Modelling of flash pyrolysis of a single wood particle. *Chemical Engineering and Processing: Process Intensification*, 39(3):239-252, 2000.
19. Salehi, E., Abedi, J., and Harding, T. Bio-oil from sawdust: effect of operating parameters on the yield and quality of pyrolysis products. *Energy & Fuels*, 25 4145-4154, 2011.
20. Yorgun, S., Şensöz, S., and Koçkar, Ö. M. Characterization of the pyrolysis oil produced in the slow pyrolysis of sunflower-extracted bagasse. *Biomass and Bioenergy*, 20(2): 141-148, 2001.
21. Pütün, A. E., Apaydin, E., and Pütün, E. Bio-oil production from pyrolysis and steam pyrolysis of soybean-cake: product yields and composition. *Energy*, 27(7):703-713, 2002.
22. Valliyappan, T., Bakhshi, N. N., and Dalai, A. K. Pyrolysis of glycerol for the production of hydrogen or syngas. *Bioresource Technology*, 99(10):4476-4483, 2008.
23. Mohan, D., Pittman Jr, C. U., and Steele, P. H. Pyrolysis of wood/biomass for biooil: a critical review. *Energy & Fuels*, 20(3):848-889, 2006.
24. Van de Velden, M., Baeyens, J., Brems, A., Janssens, B., and Dewil, R. Fundamentals, kinetics and endothermicity of the biomass pyrolysis reaction. *Renewable Energy*, *35*(1): 232-242, 2010.
25. Bridgwater, A. V. Review of fast pyrolysis of biomass and product upgrading. *Biomass and Bioenergy*, 38: 68-94, 2012.
26. Heo, H. S., Park, H. J., Park, Y. K., Ryu, C., Suh, D. J., Suh, Y. W., Yim, J. H., and Kim, S. S. Bio-oil production from fast pyrolysis of waste furniture sawdust in a fluidized bed. *Bioresource Technology*, 101(1): S91-S96, 2010.
27. Park, H.J., et al. Pyrolysis characteristics of Oriental white oak: Kinetic study and fast pyrolysis in a fluidized bed with an improved reaction system. *Fuel Processing Technology*, 90 (2), 186-195, 2009.
28. Garcia-Perez, M., Wang, X. S., Shen, J., Rhodes, M. J., Tian, F., Lee, W. J., Wu, H., and Li, C. Z. Fast pyrolysis of oil mallee woody biomass: effect of temperature on the yield and quality of pyrolysis products. *Industrial& Engineering Chemistry Research*, 47(6):1846-1854, 2008.
29. Sisto, W. J. D., Hill, N., Beis, S. H., Mukkamala, S., Joseph, J., Baker, C., Ong, T. H., Stemmler, E. A., Wheeler, M. C., Frederick, B. G., and Heiningen, A. V.

Fast pyrolysis of pine sawdust in a fluidized-bed reactor. *Energy & Fuels*, 24:2642-2651, 2010.

30. Keiluweit, M., Nico, P.S., Johnson, M.G., and Kleber, M. Dynamic molecular structure of plant biomass-derived black carbon (biochar). *Environmental Science & Technology*, 44:1247-1253, 2010.
31. Demirbas, A. Effects of temperature and particle size on bio-char yield from pyrolysis of agricultural residues. *Journal of Analytical and Applied Pyrolysis*, *72*(2), 243-248, 2004.
32. Cao, X., and Harris, W. Properties of dairy-manure-derived biochar pertinent to its potential use in remediation. *Bioresource Technology*, 101(14):5222–5228, 2010.
33. Tripathi, M., Sahu, J. N., and Ganesan, P. Effect of process parameters on production of biochar from biomass waste through pyrolysis: a review. *Renewable and Sustainable Energy Reviews*, 55:467-481, 2016.
34. Li, J., Yan, R., Xiao, B., Wang, X., and Yang, H. Influence of temperature on the formation of oil from pyrolyzing palm oil wastes in a fixed bed reactor. *Energy & fuels*, 21(4):2398-2407, 2007.
35. Shen, D. K., and Gu, S. The mechanism for thermal decomposition of cellulose and its main products. *Bioresource Technology*, 100(24):6496-6504, 2009
36. Varma, A. K., and Mondal, P. Pyrolysis of sugarcane bagasse in semi batch reactor: effects of process parameters on product yields and characterization of products. *Industrial Crops and Products*, 95:704-717, 2017.
37. Jindarom, C., Meeyoo, V., Kitiyanan, B., Rirksomboon, T., and Rangsunvigit, P. Surface characterization and dye adsorptive capacities of char obtained from pyrolysis/gasification of sewage sludge. *Chemical Engineering*, 133:239-246, 2007.
38. Inyang, M., Gao, B., Pullammanappallil, P., Ding, W., and Zimmerman, A. R. Biochar from anaerobically digested sugarcane bagasse. *Bioresource Technology*, 101:8868-8872, 2010.
39. Yao, Y., Gao, B., Inyang, M., Zimmerman, A. R., Cao, X., Pullammanappallil, P., and Yang, L. Biochar derived from anaerobically digested sugar beet tailings: characterization and phosphate removal potential. *Bioresource Technology*, 102:6273-6278, 2011.

40. Angin, D. Effect of pyrolysis temperature and heating rate on biochar obtained from pyrolysis of safflower seed press cake. *Bioresource Technology*, 128:593-597, 2013.
41. Chen, X., Chen, G., Chen, L., Chen, Y., Lehmann, J., McBride, M. B., and Hay, A. G. Adsorption of copper and zinc by biochars produced from pyrolysis of hardwood and corn straw in aqueous solution. *Bioresource Technology*, 102(19):8877-8884, 2011.
42. Chun, Y., Sheng, G., Chiou, C. T., and Xing, B. Compositions and sorptive properties of crop residue-derived chars. *Environmental Science & Technology*, 38(17):4649-4655, 2004.
43. Caglar, A., and Aydinli, B. The pyrolysis of industrial alliaceous plant wastes: illustration of process and characterization of products. *Energy Exploration & Exploitation*, 36(6), 1692-1707, 2018.
44. Xiao, R., and Yang, W. Influence of temperature on organic structure of biomass pyrolysis products. *Renewable Energy*, 50: 136-141, 2013.
45. Gibbins-Matham, J. & Kandiyoti, R. Coal pyrolysis yields from fast and slow heating in a wire-mesh apparatus with a gas sweep. *Energy & Fuels*, 2 (4), 505-511, 1988.
46. Seebauer, V., Petek, J., and Staudinger, G. Effects of particle size, heating rate and pressure on measurement of pyrolysis kinetics by thermogravimetric analysis. *Fuel*, 76(13):1277-1282, 1997.
47. Strezov, V., Moghtaderi, B., and Lucas, J.A. Thermal study of decomposition of selected biomass samples. *Journal of Thermal Analysis and Calorimetry*, 72 (3), 1041-1048, 2003.
48. Uzun, B. B., Pütün, A. E., and Pütün, E. Fast pyrolysis of soybean cake: product yields and compositions. *Bioresource Technology*, 97(4):569-576, 2006.
49. Tsai, W.T., Lee, M.K., and Chang, Y.M. Fast pyrolysis of rice husk: Product yields and compositions. *Bioresource Technology*, 98 (1), 22-28, 2007.
50. Pütün, A. E., Özbay, N., Apaydın Varol, E., Uzun, B. B., & Ateş, F. (2007). Rapid and slow pyrolysis of pistachio shell: effect of pyrolysis conditions on the product yields and characterization of the liquid product. *International journal of energy research*, *31*(5), 506-514, 2007.

51. Sensoz, S. and Angin, D. Pyrolysis of safflower (*Charthamus tinctorius* L.) seed press cake: part 1. The effects of pyrolysis parameters on the product yields. *Bioresource Technology*, 99 (13), 5492-7, 2008.
52. Debdoubi, A., El Amarti, A., Colacio, E., Blesa, M. J., and Hajjaj, L. H. The effect of heating rate on yields and compositions of oil products from esparto pyrolysis. *International journal of energy research*, *30*(15), 1243-1250, , 2006.
53. Haykiri-Acma, H., Yaman, S., and Kucukbayrak, S. Effect of heating rate on the pyrolysis yields of rapeseed. *Renewable Energy*, 31 (6), 803-810, 2006.
54. Alhumade, H., da Silva, J. C. G., Ahmad, M. S., Çakman, G., Yıldız, A., Ceylan, S., and Elkamel, A. Investigation of pyrolysis kinetics and thermal behavior of Invasive Reed Canary (Phalaris arundinacea) for bioenergy potential. *Journal of Analytical and Applied Pyrolysis*, 140, 385-392, 2019.
55. Mlonka-Mędrala, A., Evangelopoulos, P., Sieradzka, M., Zajemska, M., and Magdziarz, A. Pyrolysis of agricultural waste biomass towards production of gas fuel and high-quality char: Experimental and numerical investigations. *Fuel*, 296, 120611, 2021.
56. Aysu, T., and Küçük, M. M. Biomass pyrolysis in a fixed-bed reactor: effects of pyrolysis parameters on product yields and characterization of products. *Energy*, 64:1002-1025, 2014.
57. Ozbay, N., Pütün, A. E., and Pütün, E. Bio-oil production from rapid pyrolysis of cottonseed cake: product yields and compositions. *International Journal of Energy Research*, 30(7):501-510, 2006.
58. Kabakcı, S. B., and Baran, S. S. Hydrothermal carbonization of various lignocellulosics: Fuel characteristics of hydrochars and surface characteristics of activated hydrochars. *Waste Management*, 100, 259-268, 2019.
59. Encinar, J.M., González, J.F., and González, J. Fixed-bed pyrolysis of *Cynara cardunculus* L. Product yields and compositions. *Fuel Processing Technology*, 68 (3), 209-222, 2000.
60. Chan, W.C.R., Kelbon, M., and Krieger-Brockett, B. Single-particle biomass pyrolysis: correlations of reaction products with process conditions. *Industrial & Engineering Chemistry Research*, 27 (12), 2261-2275, 1988.

61. Beaumont, O. and Schwob, Y. Influence of physical and chemical parameters on wood pyrolysis. *Industrial & Engineering Chemistry Process Design and Development*, 23 (4), 637-641, 1984.
62. Shen, J., Wang, X. S., Garcia-Perez, M., Mourant, D., Rhodes, M. J., and Li, C. Z. Effects of particle size on the fast pyrolysis of oil mallee woody biomass. *Fuel*, *88*(10), 1810-1817, 2009.
63. Gogoi, S., Bhuyan, N., Sut, D., Narzari, R., Gogoi, L., and Kataki, R. Agricultural wastes as feedstock for thermo-chemical conversion: products distribution and characterization. *Energy Recovery Processes from Wastes*, 115-128, 2020.
64. Fan, H., Chang, X., Wang, J., and Zhang, Z.. Catalytic pyrolysis of agricultural and forestry wastes in a fixed-bed reactor using K2CO3 as the catalyst. *Waste Management & Research*, 38(1), 78-87, 2020.
65. Maggi, R. and Delmon, B. Comparison between 'slow' and 'flash' pyrolysis oils from biomass. *Fuel*, 73 (5), 671-677, 1994.
66. Putun, A.E., Apaydin, E., and Putun, E. Rice straw as a bio-oil source via pyrolysis and steam pyrolysis. *Energy*, 29 (12-15), 2171-2180, 2004.
67. Acıkgoz, C., Onay, O., and Kockar, O.M. Fast pyrolysis of linseed: product yields and compositions. *Journal of Analytical and Applied Pyrolysis*, 71 (2), 417-429, 2004.
68. Demiral, İ. and Şensöz, S. Fixed-bed pyrolysis of hazelnut (*Corylus avellana* L.) bagasse: influence of pyrolysis parameters on product yields. *Energy Sources, Part A: Recovery, Utilization, and Environmental Effects*, *28*(12), 1149-1158, 2006.
69. Widiyannita, A. M., Cahyono, R. B., Budiman, A., Sutijan, S., and Akiyama, T. Study of Pyrolysis of Ulin Wood Residues. In *AIP Conference Proceedings*, Volume 1755, Number. 1. AIP Publishing, 2016. https://doi.org/10.1063/1.4958487
70. Mohammad, I., Abakr, Y., Kabir, F., Yusuf, S., Alshareef, I. and Chin, S.,. Pyrolysis of Napier grass in a fixed bed reactor: effect of operating conditions on product yields and characteristics. *BioResources*, *10*(4), 6457-6478, 2015.
71. Yang, T., Yuan, G., Xia, M., Mu, M., and Chen, S.. Kinetic analysis of the pyrolysis of wood/inorganic composites under non-isothermal conditions. *European Journal of Wood and Wood Products*, 79, 273-284, 2021.

72. Deb, U., Bhuyan, N., Bhattacharya, S. S., and Kataki, R. . Characterization of agro-waste and weed biomass to assess their potential for bioenergy production. *International Journal of Renewable Energy Development*, 8(3), 2019.
73. Sahu, A., Sen, S., and Mishra, S. C. Processing and properties of *Calotropis gigantea* bio-char: a wasteland weed. *Materials Today: Proceedings*, 33, 5334-5340, 2020.
74. Ferreira, A. F., Dias, A. S., Silva, C. M., and Costa, M. Bio-oil and bio-char characterization from microalgal biomass. *Carbon*, 47: 99-104, 2014.
75. Shafiq, M., and Capareda, S. C. Effect of different temperatures on the properties of pyrolysis products of *Parthenium hysterophorus*. *Journal of Saudi Chemical Society*, 25(3), 101197, 2021.
76. Carsky, M., and Kuwornoo, D.K. Neural network modelling of coal pyrolysis. *Fuel* 80(7):1021–1027, 2001.
77. Sinha, S., Jhalani, A., Ravi, M. R., and Ray, A. Modelling of pyrolysis in wood: A review. *SESI Journal*, 10(1): 41-62, 2000.
78. Lee C.K., Chaiken R.F. and Singer J.M. Charring Pyrolysis of Wood in Fires by Laser Simulation. 16th Symposium (Intl.) on Combustion, Combustion Institute, Pitts: 1459-1470, 1976.
79. Yang, H., Yan, R., Chen, H., Lee, D. H., and Zheng, C. Characteristics of hemicellulose, cellulose and lignin pyrolysis. *Fuel*, 86(12-13): 1781-1788, 2007.
80. Conesa, J.A., Caballero, J.A., and Reyes-Labarta, J.A. Artificial neural network for modelling thermal decompositions. *Journal of Analytical and Applied Pyrolysis*, 71(1):343–352, 2004.
81. Angın, D., and Tiryaki, A. E. Application of response surface methodology and artificial neural network on pyrolysis of safflower seed press cake. *Energy Sources, Part A: Recovery, Utilization, and Environmental Effects*, 38(8): 1055-1061, 2016.
82. Samuel, O. D., and Okwu, M. O. Comparison of response surface methodology (RSM) and artificial neural network (ANN) in modelling of waste coconut oil ethyl esters production. *Energy Sources, Part A: Recovery, Utilization, and Environmental Effects*, *41*(9), 1049-1061, 2019.
83. Betiku, E., Adepoju, T. F., Omole, A. K., and Aluko, S. E. Statistical approach to the optimization of oil extraction from beniseed (Sesamum indicum) oilseeds. *Journal of Food Science and Engineering*, *2*(6), 351, 2012.

84. Esonye, C., Onukwuli, O. D., Ofoefule, A. U., and Ogah, E. O. (2019). Multi-input multi-output (MIMO) ANN and Nelder-Mead's simplex based modeling of engine performance and combustion emission characteristics of biodiesel-diesel blend in CI diesel engine. *Applied Thermal Engineering*, *151*, 100-114, 2019.
85. Vispute, T. P., Zhang, H., Sanna, A., Xiao, R. and Huber, G. W. Renewable chemical commodity feedstocks from integrated catalytic processing of pyrolysis oils. *Science*, 330(6008): 1222-1227, 2010.
86. Meier, D., and Faix, O. State of the art of applied fast pyrolysis of lignocellulosic materials—a review. *Bioresource Technology*, 68(1): 71-77, 1999.
87. Gonzalez-Aguilar, A. M., Cabrera-Madera, V. P., Vera-Rozo, J. R., & Riesco-Ávila, J. M. (2022). Effects of heating rate and temperature on the thermal pyrolysis of expanded polystyrene post-industrial waste. *Polymers*, *14*(22), 4957, 2022. –
88. Suriapparao, D.V., and Vinu, R. Effects of biomass particle size on slow pyrolysis kinetics and fast pyrolysis product distribution. Waste and Biomass Valorization, 9: 465–477, 2018.
89. Desai, K. M., Survase, S. A., Saudagar, P. S., Lele, S. S., and Singhal, R. S. Comparison of artificial neural network (ANN) and response surface methodology (RSM) in fermentation media optimization: case study of fermentative production of scleroglucan. *Biochemical Engineering Journal*, *41*(3), 266-273, 2008.
90. Uçar, S., and Karagöz, S. The slow pyrolysis of pomegranate seeds: the effect of temperature on the product yields and bio-oil properties. *Journal of Analytical and Applied Pyrolysis*, 84(2):151-156, 2009.
91. Nayan, N. K., Kumar, S., and Singh, R. K. Characterization of the liquid product obtained by pyrolysis of karanja seed. *Bioresource Technology*, 124: 186-189, 2012.
92. Nayan, N.K., Kumar, S., and Singh, R.K. Production of the liquid fuel by thermal pyrolysis of neem seed. *Fuel*, 103: 437–443, 2013
93. Baş, D., and Boyacı, İ. H. Modeling and optimization I: Usability of response surface methodology. *Journal of food engineering*, *78*(3), 836-845, 2007.
94. Park, H.C., Lee, B.K., Yoo, H.S. and Choi, H.S. Influence of operating conditions for fast pyrolysis and pyrolysis oil production in a conical spouted-bed reactor. *Chemical Engineering & Technology*, *42*(12), pp.2493-2504, 2019.

95. Hu, Z., Zhou, T., Tian, H., Feng, L., Yao, C., Yin, Y., and Chen, D. Effects of pyrolysis parameters on the distribution of pyrolysis products of Miscanthus. *Progress in Reaction Kinetics and Mechanism*, 46, 14686783211010970, 2021.
96. Muradov, N., Fidalgo, B., Gujar, A.C., Garceau, N., and T-Raissi, A. Production and characterization of Lemna minor bio-char and its catalytic application for biogas reforming. *Biomass & Bioenergy*, 42:123–131, 2012.
97. Promdee, K., and Vitidsant, T. Bio-oil synthesis by pyrolysis of cogongrass (*Imperata Cylindrica*). *Chemistry and Technology of Fuels and Oils*, 49(4):287-292, 2013.
98. Gusain, R., and Suthar, S. Potential of aquatic weeds (*Lemna gibba, Lemna minor, Pistia stratiotes* and *Eichhornia sp*.) in biofuel production. *Process Safety and Environmental Protection*, 109:233-241, 2017.
99. Bhattacharjee, N., and Biswas, A. B. Pyrolysis of *Alternanthera philoxeroides* (alligator weed): Effect of pyrolysis parameter on product yield and characterization of liquid product and biochar. *Journal of the Energy Institute*, 91(4):605-618, 2018.
100. Saikia, R., Chutia, R. S., Kataki, R., and Pant, K. K. Perennial grass (*Arundo donax* L.) as a feedstock for thermo-chemical conversion to energy and materials. Bioresource technology, 188, 265-272, 2015.
101. Bhattacharjee, N., and Biswas, A. B. Pyrolysis of *Ageratum conyzoides* (goat weed) Parametric influence on the product yield and product characterization. *Journal of Thermal Analysis and Calorimetry*, 139, 1515-1536, 2020.
102. Durak, H. Pyrolysis of *Xanthium strumarium* in a fixed bed reactor: Effects of boron catalysts and pyrolysis parameters on product yields and character. *Energy Sources, Part A: Recovery, Utilization, and Environmental Effects*, *38*(10), 1400-1409, 2016.
103. Radhaboy, G., Pugazhvadivu, M., Ganeshan, P., and Raja, K. Influence of kinetic parameters on *Calotropis procera* by TGA under pyrolytic conditions. *Energy Sources Part A-Recovery Utilization and Environmental Effects, 45*(3), 8257–8270, 2019.
104. Kim, J. H., Jung, S., Lin, K. Y. A., Rinklebe, J., and Kwon, E. E. Comparative study on carbon dioxide-cofed catalytic pyrolysis of grass and woody biomass. *Bioresource Technology*, 323, 124633, 2021.

105. Mishra, R. K., Lu, Q., and Mohanty, K. Thermal behaviour, kinetics and fast pyrolysis of *Cynodon dactylon* grass using Py-GC/MS and Py-FTIR analyser. *Journal of Analytical and Applied Pyrolysis*, 150, 104887, 2020.
106. Mundike, J., Collard, F. X., and Görgens, J. F. Pyrolysis of *Lantana camara* and *Mimosa pigra*: Influences of temperature, other process parameters and incondensable gas evolution on char yield and higher heating value. *Bioresource technology*, 243, 284-293, 2017.
107. Sahoo, A., Kumar, S., Kumar, J., and Bhaskar, T. A detailed assessment of pyrolysis kinetics of invasive lignocellulosic biomasses (*Prosopis juliflora* and *Lantana camara*) by thermogravimetric analysis. *Bioresource Technology*, 319, 124060, 2021.
108. Zeng, X., Xiao, Z., Zhang, G., Wang, A., Li, Z., Liu, Y., ... and Zou, D. Speciation and bioavailability of heavy metals in pyrolytic biochar of swine and goat manures. *Journal of Analytical and Applied Pyrolysis*, *132*, 82-93, 2018.
109. Azuara, M., Kersten, S. R., and Kootstra, A. M. J. Recycling phosphorus by fast pyrolysis of pig manure: concentration and extraction of phosphorus combined with formation of value-added pyrolysis products. *Biomass and bioenergy*, 49, 171-180, 2013.
110. Chong, C.T., Mong, G.R., Ng, J.-H., Chong, W.W.F., Ani, F.N., Lam, S.S., and Ong, H.C., Pyrolysis characteristics and kinetic studies of horse manure using thermogravimetric analysis. *Energy Conversion and Management*. 180, 1260–1267, 2019.
111. Yıldız, Z., Kaya, N., Topcu, Y., and Uzun, H. Pyrolysis and optimization of chicken manure wastes in fluidized bed reactor: CO2 capture in activated bio-chars. *Process Safety and Environmental Protection*, *130*, 297-305, 2019.
112. Kaur, L., Singh, J., Gayathri, G., and Negi, B. Thermogravimetric characterization of cattle manure as pyrolysis and combustion feedstocks. *International Journal of Current Microbiology and Applied Sciences.*, *11*: 2228-2237, 2020.
113. Yacob, T. W., Linden, K. G., and Weimer, A. W. Pyrolysis of human feces: Gas yield analysis and kinetic modeling. *Waste management*, *79*, 214-222, 2018.
114. Wu, Q., Wang, H., Zheng, X., Liu, F., Wang, A., Zou, D., ... and Xiao, Z., Thermochemical liquefaction of pig manure: Factors influencing on oil. *Fuel*, *264*, 116884, 2020.

115. Zhang, J., Huang, B., Chen, L., Li, Y., Li, W., and Luo, Z. Characteristics of biochar produced from yak manure at different pyrolysis temperatures and its effects on the yield and growth of highland barley. *Chemical Speciation & Bioavailability*, *30*(1), 57-67, 2018.
116. Fernandez, M. E. L., Tomasek, S., Fáyköd, C., and Somogyi, A. Investigation of the pyrolysis of animal manure in a laboratory-scale tubular reactor: the effect of the process temperature and residence time. *Hungarian Journal of Industry and Chemistry*, *50*(2), 27-33, 2022.
117. Varma, A. K., and Mondal, P. Pyrolysis of pine needles: effects of process parameters on products yield and analysis of products. *Journal of Thermal Analysis and Calorimetry*, 131, 2057-2072, 2018.
118. Lira, T. S., Santos, K. G., Murata, V. V., Gianesella, M., and Barrozo, M. A. The use of nonlinearity measures in the estimation of kinetic parameters of sugarcane bagasse pyrolysis. *Chemical Engineering & Technology*, *33*(10), 1699-1705, 2010.
119. Cai, J., Xu, D., Dong, Z., Yu, X., Yang, Y., Banks, S. W., and Bridgwater, A. V., Processing thermogravimetric analysis data for isoconversional kinetic analysis of lignocellulosic biomass pyrolysis: Case study of corn stalk. *Renewable and Sustainable Energy Reviews*, *82*, 2705-2715, 2018.
120. Garson, D.G. Interpreting neural network connection weights. *AI Expert* 6:47–51, 1991.
121. Niaei, A., Towfighi, J., Khataee, A. R., and Rostamizadeh, K. The use of ANN and the mathematical model for prediction of the main product yields in the thermal cracking of naphtha. *Petroleum science and technology*, *25*(8), 967-982, 2007.
122. Radojević, M., Janković, B., Jovanović, V., Stojiljković, D., Manić, N. Comparative pyrolysis kinetics of various biomasses based on model-free and DAEM approaches improved with numerical optimization procedure. PLoS One 13(10):e0206657, 2018.
123. Aboyade, A. O., Hugo, T. J., Carrier, M., Meyer, E. L., Stahl, R., Knoetze, J. H., and Görgens, J. F., Non-isothermal kinetic analysis of the devolatilization of corn cobs and sugar cane bagasse in an inert atmosphere. *Thermochimica Acta*, *517*(1-2), 81-89, 2011.

124. Alves, J. L. F., Da Silva, J. C. G., da Silva Filho, V. F., Alves, R. F., de Araujo Galdino, W. V., Andersen, S. L. F., and De Sena, R. F. Determination of the bioenergy potential of Brazilian pine-fruit shell via pyrolysis kinetics, thermodynamic study, and evolved gas analysis. *BioEnergy research*, *12*, 168-183, 2019.
125. Sukumar, V., Sivaprakasam, S., and Manieniyan, V. Optimization studies on bio oil production from sweet lime empty fruit bunch by pyrolysis using response surface methodology. *International Journal of Engineering Trends and Technology* (IJETT) –25 (4): 196-201, 2015.
126. Kılıç, M., Pütün, E., and Pütün, A. E. Optimization of Euphorbia rigida fast pyrolysis conditions by using response surface methodology. *Journal of Analytical and Applied Pyrolysis*, 110: 163-171, 2014.
127. Isa, K. M., Daud, S., Hamidin, N., Ismail, K., Saad, S. A., and Kasim, F. H. Thermogravimetric analysis and the optimisation of bio-oil yield from fixed-bed pyrolysis of rice husk using response surface methodology (RSM). *Industrial Crops and Products*, 33(2): 481-487, 2011.
128. Cheng, Y.-T. and Huber, G.W. Chemistry of furan conversion into aromatics and olefins over HZSM-5: A model biomass conversion reaction. *ACS Catalysis*, 1 (6), 611-628, 2011.
129. Carlson, T. R., Tompsett, G. A., Conner, W. C., and Huber, G. W. Aromatic production from catalytic fast pyrolysis of biomass-derived feedstocks. *Topics in Catalysis*, 52 (3), 241-252, 2009.
130. Shun, T. A. N., ZHANG, Z., Jianping, S. U. N., and Qingwen, W. A. N. G. Recent progress of catalytic pyrolysis of biomass by HZSM-5. *Chinese Journal of Catalysis*, *34*(4), 641-650, 2013.
131. Thring, R.W., Katikaneni, S.P.R., and Bakhshi, N.N. The production of gasoline range hydrocarbons from Alcell® lignin using HZSM-5 catalyst. *Fuel Processing Technology*, 62 (1), 17-30, 2000.
132. Bridgwater, A.V. Catalysis in thermal biomass conversion. *Applied Catalysis A: General*, 116 (1-2), 5-47, 1994.
133. Huber, G.W. and Corma, A. Synergies between bio- and oil refineries for the production of fuels from biomass. *Angewandte Chemie*, 46 (38), 7184-201, 2007.

134. Jae, J., Tompsett, G. A., Foster, A. J., Hammond, K. D., Auerbach, S. M., Lobo, R. F., and Huber, G. W. Investigation into the shape selectivity of zeolite catalysts for biomass conversion. *Journal of Catalysis*, 279 (2), 257-268, 2011.
135. Biswas, B., Singh, R., Krishna, B. B., Kumar, J., and Bhaskar, T. Pyrolysis of azolla, sargassum tenerrimum and water hyacinth for production of bio-oil. *Bioresource Technology*, 242, 139-145, 2017.
136. Williams, P.T. and Horne, P.A. Analysis of aromatic hydrocarbons in pyrolytic oil derived from biomass. *Journal of Analytical and Applied Pyrolysis*, 31 (0), 15-37, 1995.
137. Misson, M., Haron, R., Kamaroddin, M. F. A., and Amin, N. A. S. Pretreatment of empty palm fruit bunch for production of chemicals via catalytic pyrolysis. *Bioresource technology*, *100*(11), 2867-2873, 2009.
138. Aguado, J., Serrano, D. P., San Miguel, G., Castro, M. C., and Madrid, S. (2007). Feedstock recycling of polyethylene in a two-step thermo-catalytic reaction system. *Journal of Analytical and Applied Pyrolysis*, *79*(1-2), 415-423, 2007.
139. Ma, Z., Troussard, E., and van Bokhoven, J.A. Controlling the selectivity to chemicals from lignin via catalytic fast pyrolysis. *Applied Catalysis A: General*, 423–424 (0), 130-136, 2012.
140. Ben, H. and Ragauskas, A.J. Pyrolysis of kraft lignin with additives. *Energy & Fuels*, 25 (10), 4662-4668, 2011.
141. Li, X., Su, L., Wang, Y., Yu, Y., Wang, C., Li, X., and Wang, Z. Catalytic fast pyrolysis of Kraft lignin with HZSM-5 zeolite for producing aromatic hydrocarbons. *Frontiers of Environmental Science & Engineering*, *6*, 295-303, 2012.
142. Mullen, C.A. and Boateng, A.A. Catalytic pyrolysis-GC/MS of lignin from several sources. *Fuel Processing Technology*, 91 (11), 1446-1458, 2010.
143. Zhao, Y., Deng, L., Liao, B., Fu, Y., and Guo, Q. X. Aromatics production via catalytic pyrolysis of pyrolytic lignins from bio-oil. *Energy & Fuels*, *24*(10), 5735-5740, 2010.
144. Santos, L. O., Silva, F. F., Santos, L. C., Carregosa, I. S., and Wisniewski Jr, A. Potential bio-oil production from invasive aquatic plants by microscale pyrolysis studies. *Journal of the Brazilian Chemical Society*, 29, 151-158, 2018.

145. Miranda, A. F., Biswas, B., Ramkumar, N., Singh, R., Kumar, J., James, A., ... & Mouradov, A. Aquatic plant Azolla as the universal feedstock for biofuel production. *Biotechnology for Biofuels*, 9, 1-17, 2016.
146. Bulushev, D.A., and Ross, J.R.H. Catalysis for conversion of biomass to fuels via pyrolysis and gasification*: A review. Catalysis Today*, 171: 1–13, 2011.
147. Oasmaa, A., and Czernik, S. Fuel oil quality of biomass pyrolysis oils—State of the art for the end user. *Energy Fuels*, 13 : 914–921, 1999.
148. Maran, J.P., and Priya, B. Modeling of ultrasound assisted intensification of biodiesel production from neem (*Azadirachta indica*) oil using response surface methodology and artificial neural network. *Fuel* 143:262–267, 2015.
149. Lu, Q., Zhang, Z.F., Dong, C.Q., and Zhu, X.F. Catalytic upgrading of biomass fast pyrolysis vapors with nano metal oxides: an analytical Py-GC/MS study. *Energies*, 3: 1805-1820, 2010.
150. Zhang, H., Xiao, R., Wang, D., Zhong, Z., Song, M., Pan, Q., and He, G. Catalytic fast pyrolysis of biomass in a fluidized bed with fresh and spent fluidized catalytic cracking (FCC) catalysts. *Energy Fuels*, 23: 6199–6206, 2009.
151. French, R., and Czernik, S. Catalytic pyrolysis of biomass for biofuels production. *Fuel Processing Technology*, 91 : 25–32, 2010.
152. Park, H.J., Jeon, J.K., Suh, D.J., Suh, Y.W., Heo, H.S., and Park, Y.K. Catalytic vapor cracking for improvement of bio-oil quality. *Catalysis Surveys from Asia*, 15: 161–180, 2011.
153. Adjaye, J.D., and Bakhshi, N.N. Production of hydrocarbons by catalytic upgrading of a fast pyrolysis bio-oil. Part II: Comparative catalyst performance and reaction pathways. *Fue Processing Technology*, 45 : 185–202, 1995.
154. Vitolo, S., Bresci, B., Seggiani, M., and Gallo, M.G. Catalytic upgrading of pyrolytic oils over HZSM-5 zeolite: Behaviour of the catalyst when used in repeated upgrading-regenerating cycles. *Fuel*, 80 : 17–26, 2001.
155. Gogoi, S., Narzari, R., Bordoloi, N., Bhuyan, N., Sut, D., Gogoi, L., and Kataki, R. Influence of Temperature on Quality and Yield of Pyrolytic Products of Biofuel Process Wastes. In: Ghosh, S. (eds) Energy Recovery Processes from Wastes. 129-142, Springer, Singapore, , 2020.
156. Saikia, P., Gupta, U. N., Barman, R. S., Kataki, R., Chutia, R. S., and Baruah, B. P. 2015. Production and characterization of bio-oil produced from *Ipomoea carnea* bio-weed. *BioEnergy Research*, 8, 1212-1223, 2015.

157. Muradov, N., Fidalgo, B., Gujar, A. C., and Ali, T. . Pyrolysis of fast-growing aquatic biomass–*Lemna minor* (duckweed): Characterization of pyrolysis products. *Bioresource technology*, 101(21), 8424-8428, 2010.
158. Zhao, Y., Fu, Y., and Guo, Q.-X. Production of aromatic hydrocarbons through catalytic pyrolysis of γ-valerolactone from biomass. *Bioresource Technology*, 114 (0), 740-744, 2012.
159. Chen, N.Y., Walsh, D.E., and Koenig, L.R. Fluidized-bed upgrading of wood pyrolysis liquids and related compounds, In *Pyrolysis Oils from Biomass*, eds., American Chemical Society, 1988, 277-289.
160. Bordoloi, N., Narzari, R., Sut, D., Saikia, R., Chutia, R. S., and Kataki, R. . Characterization of bio-oil and its sub-fractions from pyrolysis of *Scenedesmus dimorphus*. *Renewable Energy*, 98, 245-253, 2016.
161. Lappas, A.A., Iliopoulou, E.F., and Kalogiannis, K. Catalysts in Biomass Pyrolysis, In Crocker, M. (Ed), *Thermochemical Conversion of Biomass to Liquid Fuels and Chemicals,* 263-287,The Royal Society of Chemistry, UK, , 2010.
162. Iliopoulou, E. F., Stefanidis, S. D., Kalogiannis, K. G., Delimitis, A., Lappas, A. A., and Triantafyllidis, K. S., Catalytic upgrading of biomass pyrolysis vapors using transition metal-modified ZSM-5 zeolite. *Applied Catalysis B: Environmental*, *127*, 281-290, 2012.
163. Gong, F., Yang, Z., Hong, C., Huang, W., Ning, S., Zhang, Z., ... and Li, Q. Selective conversion of bio-oil to light olefins: Controlling catalytic cracking for maximum olefins. *Bioresource technology*, *102*(19), 9247-9254, 2011.
164. Huang, W., Gong, F., Fan, M., Zhai, Q., Hong, C., and Li, Q. Production of light olefins by catalytic conversion of lignocellulosic biomass with HZSM-5 zeolite impregnated with 6 wt.% lanthanum. *Bioresource Technology*, 121 (0), 248-255, 2012.
165. Lu, Q., Tang, Z., Zhang, Y., and Zhu, X. F. Catalytic upgrading of biomass fast pyrolysis vapors with Pd/SBA-15 catalysts. *Industrial & Engineering Chemistry Research*, 49 (6), 2573-2580, 2010.
166. Cheng, Y. T., Jae, J., Shi, J., Fan, W., and Huber, G. W. Production of renewable aromatic compounds by catalytic fast pyrolysis of lignocellulosic biomass with bifunctional Ga/ZSM-5 catalysts. *Angewandte Chemie (International Edition)*, *51*(6), 2011.

167. Du, Z., Ma, X., Li, Y., Chen, P., Liu, Y., Lin, X., ... and Ruan, R. Production of aromatic hydrocarbons by catalytic pyrolysis of microalgae with zeolites: Catalyst screening in a pyroprobe. *Bioresource technology*, *139*, 397-401, 2013.
168. Thangalazhy-Gopakumar, S., Adhikari, S., and Gupta, R.B. Catalytic pyrolysis of biomass over H^+ZSM-5 under hydrogen pressure. *Energy & Fuels*, 26 (8), 5300-5306, 2012.
169. Veses, A., Puértolas, B., Callén, M. S., and García, T. Catalytic upgrading of biomass derived pyrolysis vapors over metal-loaded ZSM-5 zeolites: Effect of different metal cations on the bio-oil final properties. Microporous and Mesoporous Materials, 209, 189-196, 2015.
170. Vichaphund, S., Aht-ong, D., Sricharoenchaikul, V., and Atong, D. Production of aromatic compounds from catalytic fast pyrolysis of Jatropha residues using metal/HZSM-5 prepared by ion-exchange and impregnation methods. *Renewable Energy*, 79, 28-37, 2015.
171. Ma, C., Geng, J., Zhang, D., and Ning, X. Non-catalytic and catalytic pyrolysis of Ulva prolifera macroalgae for production of quality bio-oil. *Journal of the Energy Institute*, 93(1), 303-311, 2020.
172. Rahman, M. M., Chai, M., Sarker, M., and Liu, R. Catalytic pyrolysis of pinewood over ZSM-5 and CaO for aromatic hydrocarbon: Analytical Py-GC/MS study. *Journal of the Energy Institute*, 93(1), 425-435, 2020.
173. Aladin, A., Modding, B., Syarif, T. and Dewi, F.C., Effect of nitrogen gas flowing continuously into the pyrolysis reactor for simultaneous production of charcoal and liquid smoke. In *Journal of Physics: Conference Series* (Vol. 1763, No. 1, p. 012020). IOP Publishing, 2021.
174. Saif, A. G. H., Wahid, S. S., and Ali, M. R.. Pyrolysis of sugarcane bagasse: the effects of process parameters on the product yields. In *Materials Science Forum*, Vol. 1008, pp. 159-167, Trans Tech Publications Ltd, 2020.
175. Dada, T. K., Sheehan, M., Murugavelh, S., and Antunes, E. A review on catalytic pyrolysis for high-quality bio-oil production from biomass. *Biomass Conversion and Biorefinery*, *13*(4), 2595-2614, 2023.
176. Basu, P. Biomass Gasification and Pyrolysis – Practical Design and Theory (1st ed.), Academic Press, Burlington, 2010.

177. Vassilev, S. V., Baxter, D., Andersen, L. K., Vassileva, C. G., and Morgan, T. J. An overview of the organic and inorganic phase composition of biomass. *Fuel*, 94: 1-33, 2012.
178. Hemberger, P., Custodis, V. B., Bodi, A., Gerber, T., and van Bokhoven, J. A.. Understanding the mechanism of catalytic fast pyrolysis by unveiling reactive intermediates in heterogeneous catalysis. *Nature communications*, *8*(1), 1-9, 2017.
179. Liu, R., Rahman, M. M., Sarker, M., Chai, M., Li, C., and Cai, J. A review on the catalytic pyrolysis of biomass for the bio-oil production with ZSM-5: Focus on structure. *Fuel Processing Technology*, *199*, 106301, 2020.
180. Mihalcik, D. J., Mullen, C. A., and Boateng, A. A. Screening acidic zeolites for catalytic fast pyrolysis of biomass and its components. *Journal of Analytical and Applied Pyrolysis*, *92*(1), 224-232, 2011.
181. Basumatary, V., Saikia, R., Narzari, R., Bordoloi, N., Gogoi, L., Sut, D., ... and Kataki, R. Tea factory waste as a feedstock for thermo-chemical conversion to biofuel and biomaterial. *Materials Today: Proceedings*, 5(11), 23413-23422, 2018.
182. Choudhury, N. D., Bhuyan, N., Bordoloi, N., Saikia, N., and Kataki, R. . Production of bio-oil from coir pith via pyrolysis: kinetics, thermodynamics, and optimization using response surface methodology. *Biomass Conversion and Biorefinery*, 11, 2881-2898, 2021.
183. Chutia, S., Narzari, R., Bordoloi, N., Saikia, R., Gogoi, L., Sut, D., ... and Kataki, R. Pyrolysis of dried black liquor solids and characterization of the bio-char and bio-oil. *Materials Today: Proceedings*, 5(11), 23193-23202, 2018.
184. Choudhury, N. D., Chutia, R. S., Bhaskar, T., and Kataki, R. Pyrolysis of jute dust: effect of reaction parameters and analysis of products. *Journal of Material Cycles and Waste Management*, 16, 449-459, 2014.
185. Holubčík, M., Klačko, A., Jandačka, J., and Drga, J. . Pyrolysis Treatment of Municipal Solid Waste and Automotive Waste with Study of Each Component Energy Potential. In MATEC Web of Conferences (Vol. 369, p. 03005). EDP Sciences, 2022.
186. Chen, X., Wu, R., Sun, Y., and Jian, X. Synergistic effects on the co-pyrolysis of agricultural wastes and sewage sludge at various ratios. *ACS Omega*, 7(1), 1264-1272, 2021.

187. Dash, M., Venkata Dasu, V., Mohanty, K. Physico-chemical characterization of *Miscanthus, Castor*, and *Jatropha* towards biofuel production. *Journal of Renewable and Sustainable Energy*, 7(4), 043124, 2015.
188. Shadangi, K.P., Mohanty, K. Characterization of nonconventional oil containing seeds towards the production of bio-fuel. *Journal of Renewable and Sustainable Energy*,5(3), 033111, 2013.
189. Saeed, S., Ashour, I., Sherif, H., Ali, M. R. Catalytic and noncatalytic fast pyrolysis of Jatropha seeds: Experimental measurements and modeling. *Egyptian Journal of Chemistry*., 63(2), 683-702, 2020.
190. Doshi, P., Srivastava, G., Pathak, G., and Dikshit, M. Physicochemical and thermal characterization of nonedible oilseed residual waste as sustainable solid biofuel. *Waste Management* 34(10), 1836, 2014.
191. Box, G. E. P., Hunter, W. G., and Hunter, J. S. Statistics for Experimenters: An Introduction to Design, Data Analysis and Model Building. John Wiley and Sons Inc., Pages: 653, ISBN-13: 9780471093152, New York, USA., 1978.
192. Mishra, R. K., and Mohanty, K. Characterization of non-edible lignocellulosic biomass in terms of their candidacy towards alternative renewable fuels. *Biomass Conversion and Biorefinery* 8(4), 799, 2018.
193. Sut, D., Chutia, R. S., Bordoloi, N., Narzari, R., and Kataki, R. Complete utilization of non-edible oil seeds of *Cascabela thevetia* through a cascade of approaches for biofuel and by-products. *Bioresource Technology*, 213, 111-120, 2016.
194. Kumar, A., Wang, L., Dzenis, Y.A., Jones, D. D., and Hanna, M.A. Thermogravimetric characterization of corn stover as gasification and pyrolysis feedstock. *Biomass and Bioenergy*, 32 :460 – 467, 2008.
195. Jeguirim, M., and Trouve, G. Pyrolysis characteristics and kinetics of *Arundo donax* using thermogravimetric analysis. *Bioresource Technology*, 100 : 4026–4031, 2009.
196. Li, D., Chen, L., Yi, X., Zhang, X., and Ye, N. Pyrolytic characteristics and kinetics of two brown algae and sodium alginate. *Bioresource Technology*, 101 : 7131–7136, 2010.
197. Chutia, R. S., Kataki, R., and Bhaskar, T. Thermogravimetric and decomposition kinetic studies of *Mesua ferrea* L. deoiled cake. *Bioresource Technology*, 139, 66-72, 2013.

198. Bordoloi, N., Narzari, R., Chutia, R.S., Bhaskar, T., Kataki, R., Pyrolysis of *Mesua ferrea* and *Pongamia glabra* seed cover: Characterization of bio-oil and its sub-fractions, *Bioresource Technology 178*, 83-89, 2015.
199. Sanchez-Jimenez, P.E., Perez-Maqueda, L.A., Perejon, A., and Criado, J.M. Generalized master plots as a straightforward approach for determining the kinetic model: The case of cellulose pyrolysis. *Thermochimica Acta*, 552: 54– 59, 2013.
200. Kusworo, T. D., Widayat, W., Mahadita, A. F., Firizqina, D., and Utomo, D. P. (2020). Bio-oil and fuel gas production from agricultural waste via pyrolysis: a comparative study of oil palm empty fruit bunches (OPEFB) and rice husk. *Periodica Polytechnica Chemical Engineering*, 64(2), 179-191, 2020.
201. Raj, T., Kapoor, M., Gaur, R., Christopher, J., Lamba, B., Tuli, D. K., and Kumar, R. Physical and chemical characterization of various Indian agriculture residues for biofuels production. *Energy & Fuels*, *29*(5), 3111-3118, 2015.
202. Mishra, G., Kumar, J., and Bhaskar, T. Kinetic studies on the pyrolysis of pinewood. *Bioresource Technology*, 182 : 282–288, 2015.
203. Montgomery, D.C. Design and Analysis of Experiments. John Wiley and Sons, 5th edition, New York, 2001.
204. Collazzo, G.C., Broetto, C.C., Perondi, D., Junges, J., Dettmer, A., Filho, A.A.D., Foletto, E.L., and Godinho, M. A detailed non-isothermal kinetic study of elephant grass pyrolysis from different models. *Applied Thermal Engineering*, 110 : 1200–1211, 2017.
205. Gogoi, M., Konwar, K., Bhuyan, N., Borah, R.C., Kalita, A.C., Nath, H.P., and Saikia, N. Assessments of pyrolysis kinetics and mechanisms of biomass residues using thermogravimetry. *Bioresource Technology Reports*, 4 : 40–49, 2018.
206. Brasil, J. L., Martins, L. C., Ev, R. R., Dupont, J., Dias, S. L., Sales, J. A., Airoldi, C., and Lima, É. C. Factorial design for optimization of flow-injection preconcentration procedure for copper (II) determination in natural waters, using 2- aminomethylpyridine grafted silica gel as adsorbent and spectrophotometric detection. *International Journal of Environmental Analytical Chemistry*, 85(7):475- 491, 2005.
207. Muravyev, N.V., and Pivkina, A.N. New concept of thermokinetic analysis with artificial neural networks. *Thermochim Acta* 637:69–73, 2016.
208. Ahmad, M. S., Mehmood, M. A., Taqvi, S. T. H., Elkamel, A., Liu, C. G., Xu, J., ... and Gull, M. Pyrolysis, kinetics analysis, thermodynamics parameters and

reaction mechanism of *Typha latifolia* to evaluate its bioenergy potential. *Bioresource Technology*, 245, 491-501, 2017.

209. Ongpeng, J.M.C., Gapuz, E., Roxas, C.L.C. Optimizing compressed earth blocks mix design incorporating rice straw and cement using artificial neural network, 2017 IEEE 9th International Conference on Humanoid, Nanotechnology, Information Technology, Communication and Control, Environment and Management (HNICEM), Manila, pp. 1-6, 2017. https://doi.org/10.1109/HNICEM.2017.8269450

210. Xu, Y., Liu, Z., Peng, Y., You, T., and Hu, X. Catalytic pyrolysis kinetics behavior of *Chlorella pyrenoidosa* with thermal gravimetric analysis. *Journal of Renewable and Sustainable Energy*, 9(6), 063105, 2017.

211. Wang, L., Lei, H., Liu, J., and Bu, Q. Thermal decomposition behavior and kinetics for pyrolysis and catalytic pyrolysis of Douglas fir. RSC advances, 8(4), 2196-2202, 2018.

212. Abnisa, F., Daud, W. W., & Sahu, J. N. Optimization and characterization studies on bio-oil production from palm shell by pyrolysis using response surface methodology. *Biomass and Bioenergy*, *35*(8), 3604-3616, 2011.

213. Thoai, D. N., Tongurai, C., Prasertsit, K., and Kumar, A. Predictive capability evaluation of RSM and ANN in modeling and optimization of biodiesel production from palm (*Elaeis guineensis*) oil. *International Journal of Applied Engineering Research*, 13(10), 7529-7540, 2018.

214. Betiku, E., Okunsolawo, S. S., Ajala, S. O., and Odedele, O. S. Performance evaluation of artificial neural network coupled with generic algorithm and response surface methodology in modeling and optimization of biodiesel production process parameters from shea tree (*Vitellaria paradoxa*) nut butter. *Renewable Energy*, *76*, 408-417, 2015.

215. Ebrahimpour, A., Rahman, R. N. Z. R. A., Ean Ch'ng, D. H., Basri, M., & Salleh, A. B. A modeling study by response surface methodology and artificial neural network on culture parameters optimization for thermostable lipase production from a newly isolated thermophilic Geobacillus sp. strain ARM. BMC biotechnology, 8, 1-15, 2008.

216. Saikia, R., Baruah, B., Kalita, D., Pant, K. K., Gogoi, N., and Kataki, R. . Pyrolysis and kinetic analyses of a perennial grass (*Saccharum ravannae* L.) from north-

east India: optimization through response surface methodology and product characterization. *Bioresource Technology*, 253, 304-314, 2018.

217. Tripathi, M., Bhatnagar, A., Mubarak, N. M., Sahu, J. N., and Ganesan, P. . RSM optimization of microwave pyrolysis parameters to produce OPS char with high yield and large BET surface area. *Fuel*, 277, 118184, 2020.

218. Aydinli, B., Caglar, A., Pekol, S., and Karaci, A. (). The prediction of potential energy and matter production from biomass pyrolysis with artificial neural network. *Energy Exploration & Exploitation*, 35(6), 698-712, 2017.

219. Madhu, P., Matheswaran, M. M., and Periyanayagi, G. Optimization and characterization of bio-oil produced from cotton shell by flash pyrolysis using artificial neural network. *Energy Sources, Part A: Recovery, Utilization, and Environmental Effects*, 39(23), 2173-2180, 2017.

220. Yanik, J., Kornmayer, C., Saglam, M., and Yüksel, M. Fast pyrolysis of agricultural wastes: Characterization of pyrolysis products. *Fuel Processing Technology*, 88(10), 942-947, 2007.

221. Aguilar, G., D Muley, P., Henkel, C., and Boldor, D. . Effects of biomass particle size on yield and composition of pyrolysis bio-oil derived from Chinese tallow tree (*Triadica Sebifera* L.) and energy cane (Saccharum complex) in an inductively heated reactor. *Aims Energy*, *3*(4), 2015.

222. Septien, S., Valin, S., Dupont, C., Peyrot, M. and Salvador, S., Effect of particle size and temperature on woody biomass fast pyrolysis at high temperature (1000–1400 C). *Fuel*, *97*, 202-210, 2012.

223. Ahmad, M. S., Liu, C. G., Nawaz, M., Tawab, A., Shen, X., Shen, B., and Mehmood, M. A.. Elucidating the pyrolysis reaction mechanism of Calotropis procera and analysis of pyrolysis products to evaluate its potential for bioenergy and chemicals. *Bioresource Technology*, 322, 124545, 2021. .

224. Malagón Romero, D., Gómez Junca, J. S., Tinoco Navarro, L. K., and Arrubla Vélez, J. P.. Elucidating the pyrolysis properties of water hyacinth *(Eichhornia crassipes*) biomass and characterisation of its pyrolysis products. *International Journal of Sustainable Energy*, *42*(1), 72-90, 2023.

225. Aysu, T., and Durak, H. Thermochemical conversion of *Datura stramonium L.* by supercritical liquefaction and pyrolysis processes. *The Journal of Supercritical Fluids*, *102*, 98-114, 2015.

226. Oginni, O., and Singh, K. . Pyrolysis characteristics of *Arundo donax* harvested from a reclaimed mine land. *Industrial Crops and Products*, *133*, 44-53, 2019.
227. Ilo, O. P., Nkomo, S. P. L., Mkhize, N. M., Mutanga, O., and Simatele, M. D. Optimisation of process parameters using response surface methodology to improve the liquid fraction yield from pyrolysis of water hyacinth. *Environmental Science and Pollution Research*, *30*(3), 6681-6704, 2023.
228. Abnisa, F., Daud, W. W., Ramalingam, S., Azemi, M. N. B. M., and Sahu, J. N. Co-pyrolysis of palm shell and polystyrene waste mixtures to synthesis liquid fuel. *Fuel*, 108: 311-318, 2013.
229. Qurat-ul-Ain, Shafiq, M., Capareda, S. C., and Firdaus-e-Bareen . Effect of different temperatures on the properties of pyrolysis products of *Parthenium hysterophorus*. *Journal of Saudi Chemical Society*, *25*(3), 101197, 2021.
230. Jung, K. A., Nam, C. W., Woo, S. H., and Park, J. M. Response surface method for optimization of phenolic compounds production by lignin pyrolysis. *Journal of Analytical and Applied Pyrolysis*, 120: 409-415, 2016.
231. Jamaluddin, M. A., Ismail, K., Ishak, M. A. M., AbGhani, Z., Abdullah, M. F., Safian, M. T. U., Idris, S. S., Tahiruddin, S., Yunus, M.F.M., and Hakimi, N. I. N. M. Microwave-assisted pyrolysis of palm kernel shell: Optimization using response surface methodology (RSM). *Renewable Energy*, 55: 357-365, 2013.
232. Wauton, I., and Ogbeide, S. E. Characterization of pyrolytic bio-oil from water hyacinth (Eichhornia crassipes) pyrolysis in a fixed bed reactor. Biofuels, 12(8), 899–904, 2019.
233. Huang, H., Liu, J., Liu, H., Evrendilek, F., and Buyukada, M. Pyrolysis of water hyacinth biomass parts: Bioenergy, gas emissions, and by-products using TG-FTIR and Py-GC/MS analyses. *Energy Conversion and Management*, *207*, 112552, 2020.
234. Arumugasamy, S.K., Selvarajoo, A. Feedforward neural network modeling of biomass pyrolysis process for biochar production. *Chemical Engineering Transactions*. 45:1681–1686, 2015
235. Lappas, A. A., Kalogiannis, K. G., Iliopoulou, E. F., Triantafyllidis, K. S., and Stefanidis, S. D. Catalytic pyrolysis of biomass for transportation fuels. *Advances in bioenergy: the sustainability challenge*, 45-56, 2016.
236. Zhang, L., Bao, Z., Xia, S., Lu, Q., and Walters, K. B. Catalytic pyrolysis of biomass and polymer wastes. *Catalysts*, 8(12), 659, 2018.

237. Pasangulapati, V., Ramachandriya, K. D., Kumar, A., Wilkins, M. R., Jones, C. L., and Huhnke, R. L. Effects of cellulose, hemicellulose and lignin on thermochemical conversion characteristics of the selected biomass. *Bioresource Technology*, 114: 663-669, 2012.

238. Pandey, S. P., Upadhyay, R., Prakash, R., and Kumar, S. Performance and emission analysis of blends of bio-oil obtained by catalytic pyrolysis of *Argemone mexicana* seeds with diesel in a CI engine. *Environmental Science and Pollution Research*, 30, 125034–125047, 2022.